Efficient Prediction of Array Element Patterns Using Physics-Based Expansions and a Single Far-Field Measurement

Rob Maaskant, *Member, IEEE*, Marianna V. Ivashina, *Member, IEEE*, Stefan J. Wijnholds, *Member, IEEE*, and Karl F. Warnick, *Senior Member, IEEE*

Abstract—**A method is proposed to predict the antenna array beam through employing a relatively small set of physics-based basis functions—called characteristic basis function patterns (CBFPs)—for modeling the embedded element patterns. The primary CBFP can be measured or extracted from numerical simulations, while additional (secondary) CBFPs are derived from the primary one. Furthermore, each numerically generated CBFP, which is typically simulated/measured for discrete directions only, can in turn be approximated by analytical basis functions with fixed expansion coefficients to evaluate the resulting array pattern at any angle through interpolation. This hierarchical basis reduces the number of unknown expansion coefficients significantly. Accordingly, the CBFP expansion coefficients can be determined through a single far-field measurement of only a few reference sources in the field of view. This is particularly important for multibeam array applications where only a limited number of reference sources are available for predicting the beam shape. Furthermore, this instantaneous beam calibration is fast, i.e., potentially capable to speed up the array calibration by one or two orders of magnitude, which is particularly important if the antenna radiation characteristics are subject to drifts.**

Index Terms—**Beam calibration, far-field pattern, phased array antennas.**

I. INTRODUCTION

IN many antenna array applications it is vitally important to accurately measure the far-field beams as a function of angle, so as to monitor and control the side-lobe level, the beam stability and beam overlap in multibeam applications, to resolve the direction-dependent errors of interferometric imaging arrays, etc. Very fine sampling of the pattern, however, requires a long measurement time during which the system performance must be time-invariant to prevent the radiation characteristics of high-sensitivity antenna systems from drifting. Consequently, practical beam calibration becomes difficult—if not impossible—if the number of required measurement samples is large. To reduce the beam calibration time, one could measure a number of sky reference sources at once, rather than on a source-by-source basis. More specifically, we will assume that all N antenna element output ports are accessible and that their output voltages are correlated[1] to form an $N \times N$ output covariance matrix **R**. Although this complicates the beamforming network, **R** contains the information of all measured sources via a single measurement. For instance, for r perfectly-polarized incoherent sources in the sky, **R** is of rank r, that is, a sum of r rank-one matrices, one for each source. Indeed, a consecutive measurement of r output voltage vectors, one for each source, may be a time-consuming process, particularly if the antenna has to be physically rotated or the sky reference sources have to move to a different location within the field of view (FoV).

Once **R** is measured, one can employ antenna array signal processing algorithms to retrieve information about the source(s) [1], which is common practice for interferometric imaging array antennas for radio astronomy [2], MIMO communication, and radar applications. In this paper, however, our objective is to use a known set of incoherent sky reference sources to be able to identify the antenna beam pattern. Note that, even though the presented methodology is general, if only cosmic incoherent power point sources are used, the phase of the pattern cannot be calibrated for, so that we will limit ourselves to modeling the power pattern only. Research is ongoing to eliminate this so-called phase ambiguity by using additional artificial reference sources in the vicinity of the antenna whose radiated fields are known in both amplitude and phase.

Since the number of natural reference sources in the antenna's FoV may be very limited, we will employ a suitable set of complex-valued vector basis function patterns for interpolating the pattern between distant samples. Furthermore, since the basis functions should account for the array element positioning and the intrinsic physics of each radiator, we propose to employ physics-based basis function patterns (e.g. simulated ones, which account for the element geometry and obey Maxwell's equations) to limit the degrees of freedom of the pattern to those that are physically relevant. This generally

---

[1]For narrowband signals, the correlation R_{12} is obtained by first multiplying the two instantaneously measured output voltage phasors V_1 and V_2, one of which is complex conjugated, after which the relatively slowly-varying product $V_1(t)V_2^*(t)$ is estimated (time-averaged) to yield $R_{12} = \langle V_1 V_2^* \rangle$.

leads to a much smaller number of basis functions than a more general mathematical-function-based expansion alone.

It is pointed out that, over the past decade, much attention has been devoted to reducing the number of basis functions for the currents in method-of-moment approaches, so that the matrix equation can be solved in-core on standard desktop computers without compromising the solution accuracy much. These methods have not yet been applied to generate a small set of basis functions for the far-field patterns. Hence, and analogous to the characteristic basis function method for the current (CBFM, [3], [4]), we expand the practical/actual unknown embedded element pattern (EEP) of an antenna array element—thus antenna coupling included—in terms of a few discretely sampled (simulated) characteristic basis function patterns (CBFPs). The first (primary) CBFP is chosen to be the ideal EEP obtained from numerical simulations, which is supposed to be very close to the actual EEP. To further minimize the pattern modeling error, additional (secondary) CBFPs are generated which should be chosen with care as they are expected to compensate certain types of pattern errors. For example; if a manufacturing tolerance in the element geometry is to be expected, it seems natural to simulate the EEP of a few perturbed element geometries and use these as higher-order CBFPs. Hence, the methodology is general but hinges on the way higher-order CBFPs are generated. In this paper, we consider the specific case that the elements are expected to be mismatched. Thus, exciting one element in an array environment causes the output waves to reflect at the mismatched terminations, which in turn excite the elements to contribute to the radiation pattern. Hence, to compensate/model for this pattern change, it seems natural to use the EEPs of the direct neighboring antenna elements as secondary CBFPs and append it to the primary CBFP for the element under consideration. This procedure is repeated for each antenna array element, so that each antenna element supports a set of CBFPs.

Furthermore, the number of pattern expansion coefficients is kept to a minimum by neglecting array truncation effects. As a result, all EEPs are identical (apart from a phase correction) and can therefore be expanded into the same set of CBFPs (apart from a phase correction) with identical expansion coefficients. This is accurate if systematic errors in the EEP are expected for very large regular arrays—dense or sparse—but also for weakly-coupled sparse arrays, or stronger-coupled irregular arrays whenever the synthesized EEP is viewed as an *average* EEP [5]. Note that the pattern change due to mismatch effects is minimal in sparse or weakly-coupled arrays, so that we will consider strongly-coupled antenna arrays only. The methodology allows to use several CBFP expansions for several parts of the array (say central and edge elements) to model differences in EEPs from element to element. However, this would increase the degrees of freedom (number of unknown expansion coefficients) and may lead to non-unique solutions if the number of expansion coefficients becomes too large [6]. Consequently, the sources should move to other places in the field of view to perform additional independent measurements, which is undesired if the beam calibration measurement has to be performed instantaneously in order to prevent drifts in the system performance. For one expansion, only a few CBFP expansion coefficients of

a single (average) array element have to be determined, which requires an equally low amount of incoherent far-field reference sources in the antenna's FoV during the measurement. Accordingly, the expansion coefficients for the pattern are determined indirectly by least-squares fitting the modeled output covariance matrix to the measured one, following similar techniques as in phased array self-calibration [7, Ch. 5].

If desired, and without increasing the number of unknowns, each so-generated CBFP can be represented analytically by a series of mathematical basis functions with fixed expansion coefficients to ease pattern interpolation, such as the Jacobi-Bessel series [8] if the CBFPs are generated by sources distributed over a large aperture, or spherical wave functions if the CBFPs originate from localized source, etc. Expanding a pattern in terms of analytical basis functions is common practice and therefore not discussed further. The herein proposed hierarchical basis therefore expands the numerically-generated CBFPs into many lower-order ones, as opposed to employing a series expansion of analytical functions alone.

The generation of basis function patterns (CBFPs) is discussed in Section II. Afterwards, in Section III, a model is developed for the output covariance matrix, both for perfectly-polarized and unpolarized reference sources. The determination of the pattern expansion coefficients through a least-squares fitting procedure is discussed in Section IV. In Section V, numerical results are presented for an 11-element array of dipoles and strongly coupled tapered-slot antennas whose CBFPs are first extracted from an ideal numerical antenna model, after which these CBFPs are used to model the actual non-ideal array beam, which is herein simulated by summing a perturbed set of embedded element patterns. Finally, in Section VI, the solution stability of the expansion coefficients as a function of the location and distance between the reference point sources is assessed through the matrix condition number.

II. MODELING THE FAR-FIELD BEAMS

It is assumed that the actual/measured unknown E-field EEP of the pth antenna array element, $\boldsymbol{f}_p(\theta, \phi) = E_{\theta;p}(\theta, \phi)\hat{\boldsymbol{\theta}} + E_{\phi;p}(\theta, \phi)\hat{\boldsymbol{\phi}}$, at position $\boldsymbol{r}_p$ can be described by the M_p basis function patterns $\{\boldsymbol{g}_{mp}\}_{m=1}^{M_p}$, i.e.

$$\boldsymbol{f}_p(\theta, \phi) = \sum_{m=1}^{M_p} \alpha_{mp}\boldsymbol{g}_{mp}(\theta, \phi) \tag{1}$$

where $\{\alpha_{mp}\}$ are the M_p unknown complex-valued CBFP expansion coefficients for the pth antenna element. The EEP $\boldsymbol{f}_p$ arises if element p is excited by a current source of unit amplitude while all other terminals are open-circuited. The loaded case is discussed in Section IV.

As stated in the introduction, if edge-truncation effects can be neglected, all EEPs are identical, apart from a phase transformation in accordance to the translated position of the antenna element (array factor), i.e., the qth element pattern is derived from the pth reference one as

$$\boldsymbol{f}_q(\theta, \phi) = \boldsymbol{f}_p(\theta, \phi)e^{-j\boldsymbol{k}(\theta,\phi)\cdot[\boldsymbol{r}_q - \boldsymbol{r}_p]} \tag{2}$$

where the free-space wave vector is herein defined as $\boldsymbol{k}(\theta, \phi) = -(2\pi/\lambda_0)[\sin(\theta)\cos(\phi)\hat{\boldsymbol{x}} + \sin(\theta)\sin(\phi)\hat{\boldsymbol{y}} + \cos(\theta)\hat{\boldsymbol{z}}]$. Note that $[\boldsymbol{r}_q - \boldsymbol{r}_p]$ realizes a phase correction relative to the element p, instead of to the global origin of the array. Accordingly, the qth EEP is expanded as

$$\boldsymbol{f}_q(\theta, \phi) = e^{-j\boldsymbol{k}(\theta, \phi)\cdot[\boldsymbol{r}_q - \boldsymbol{r}_p]} \sum_{m=1}^{M} \alpha_m \boldsymbol{g}_m(\theta, \phi) \qquad (3)$$

for $q = 1, \ldots, N$, where we now have only M CBFP complex-valued expansion coefficients $\{\alpha_m\}$ that need to be determined.

The set of basis function patterns $\{\boldsymbol{g}_m\}$ can be determined on physical grounds. The most dominant basis function $\boldsymbol{g}_1$ (primary CBFP) is the one that is closest to the actual EEP. For this CBFP one can use the simulated (or measured) EEP extracted from a large array environment. The EEP in a real system will only be slightly perturbed from that. If this perturbation is due to slightly mismatched antennas, this change in EEP occurs because of the reflected waves at the antenna terminations that, in turn, excite the nearest antenna neighbors. Our suggestion is therefore to employ the neighboring EEPs as secondary CBFPs to be able to correct for this type of perturbation. As a result, the entire set of CBFPs for a centralized antenna element becomes

$$\{\boldsymbol{g}_m\}_{m=1}^{M} = \left\{ \boldsymbol{g}_1, \boldsymbol{g}_1 e^{-j\boldsymbol{k}(\theta, \phi)\cdot\boldsymbol{d}_1}, \ldots, \boldsymbol{g}_1 e^{-j\boldsymbol{k}(\theta, \phi)\cdot\boldsymbol{d}_M} \right\} \quad (4)$$

where the M nearest EEPs are selected, each of which is derived by applying a phase-pattern correction to $\boldsymbol{g}_1$ in accordance with the geometric offset $\boldsymbol{d}_m$ relative to the element under consideration. It is pointed out that each CBFP can be expanded in terms of a set of analytical basis functions with fixed coefficients to ease pattern interpolation.

In matrix-vector notation, and when dropping the (θ, ϕ) dependence, (3) can be written as

$$\boldsymbol{f}_q = e^{-j\boldsymbol{k}\cdot[\boldsymbol{r}_q - \boldsymbol{r}_p]} \mathbf{G}\boldsymbol{\alpha}, \quad \text{for } q = 1, \ldots, N \qquad (5)$$

where the column-augmented matrix $\mathbf{G} = [\boldsymbol{g}_1, \boldsymbol{g}_2, \cdots, \boldsymbol{g}_M]$ is of size $2 \times M$ (2 far-field components), and the $M \times 1$ column vector $\boldsymbol{\alpha} = [\alpha_1, \alpha_2, \cdots, \alpha_M]^T$, where T denotes the transposition operator. Note that, by assuming $\mathbf{G}$ constant for all array elements, the same relative offset positions of the neighboring antenna elements is assumed, which may not be true for edge elements, but this is a consequence of assuming that all EEPs are identical.

Eq. (5) provides a mathematical model for all EEPs, where $\boldsymbol{\alpha}$ is the only unknown vector that needs to be determined, which can be done through performing a single far-field measurement. More specifically, for a sky containing a number of relatively strong and incoherent far-field sources in the FoV, one commonly measures a voltage covariance matrix at the receiver outputs. Our approach is therefore to least-squares-fit the $N \times N$ modeled covariance matrix to the measured one in order to find $\boldsymbol{\alpha}$ as discussed below.

III. MODELING THE VOLTAGE COVARIANCE MATRIX

A. Far-Field Point Sources (No Noise)

The open-circuited pth output port voltage, which arises due to a deterministic perfectly-polarized plane-wave field $\boldsymbol{E}^{\mathrm{i}}(\Omega)$ incident from direction Ω, can be computed through antenna reciprocity as: $V_p^{\mathrm{oc}} = (1/j\omega\mu_0)\boldsymbol{f}_p(\Omega) \cdot \boldsymbol{E}^{\mathrm{i}}(\Omega)$ [4, p. 27]. Upon neglecting estimation error, the element R_{pq}^{oc} of the $N \times N$ output voltage covariance matrix $\mathbf{R}^{\mathrm{oc}}$ is thus computed as

$$R_{pq}^{\mathrm{oc}} = \left\langle V_p^{\mathrm{oc}} \left(V_q^{\mathrm{oc}} \right)^* \right\rangle = \frac{\left[\boldsymbol{f}_p(\Omega) \cdot \boldsymbol{E}^{\mathrm{i}}(\Omega) \right] \left[\boldsymbol{f}_q(\Omega) \cdot \boldsymbol{E}^{\mathrm{i}}(\Omega) \right]^*}{\omega^2 \mu_0^2} \qquad (6)$$

where * indicates conjugation. Substituting (5) in (6), yields

$$\begin{aligned} R_{pq}^{\mathrm{oc}} &= \frac{e^{j\boldsymbol{k}\cdot[\boldsymbol{r}_q - \boldsymbol{r}_p]}}{\omega^2 \mu_0^2} \left[(\mathbf{G}\boldsymbol{\alpha}) \cdot \boldsymbol{E}^{\mathrm{i}} \right] \left[(\mathbf{G}\boldsymbol{\alpha}) \cdot \boldsymbol{E}^{\mathrm{i}} \right]^* \\ &= \boldsymbol{\alpha}^H \left[\frac{e^{j\boldsymbol{k}\cdot[\boldsymbol{r}_q - \boldsymbol{r}_p]}}{\omega^2 \mu_0^2} \mathbf{G}^H \boldsymbol{E}^{\mathrm{i}}(\boldsymbol{E}^{\mathrm{i}})^H \mathbf{G} \right] \boldsymbol{\alpha} \\ &= \boldsymbol{\alpha}^H \mathbf{A}_{pq} \boldsymbol{\alpha} \qquad (7) \end{aligned}$$

where the matrix block $\mathbf{A}_{pq}$ is of size $M \times M$ and given as

$$\mathbf{A}_{pq} = \sum_{s=1}^{r} \frac{e^{j\boldsymbol{k}\cdot[\boldsymbol{r}_q - \boldsymbol{r}_p]}}{\omega^2 \mu_0^2} \mathbf{G}^H(\Omega_s) \boldsymbol{E}^{\mathrm{i}}(\Omega_s) \left(\boldsymbol{E}^{\mathrm{i}}(\Omega_s) \right)^H \mathbf{G}(\Omega_s) \qquad (8)$$

for r incoherent reference sources observed at the r distinct directions[2] $\Omega_1, \ldots, \Omega_r$. Note that the matrix block $\mathbf{A}_{pq}$ can be readily computed, since the basis functions and reference sources are supposed to be known. The problem is therefore to find $\boldsymbol{\alpha}$ in (7) so that R_{pq}^{oc} is modeled best in a least-squares sense $\forall p, q \in \{1, \ldots, N\}$.

B. Distributed Far-Field Sources (Noise Present)

In the more general case of distributed sources, and in the presence of noise, the statistical expectation $\mathbb{E}\{V_p^{\mathrm{oc}}(V_q^{\mathrm{oc}})^*\}$ of each voltage covariance matrix element must be estimated. Assuming that the statistical noise sources are (wide-sense) stationary random processes which exhibit ergodicity, ensemble averages may be replaced by a time average of a sufficiently long sample (realization) of the process to minimize estimation error. Hence,

$$\mathbb{E}\left\{ R_{pq}^{\mathrm{oc}} \right\} = \left\langle V_p^{\mathrm{oc}} \left(V_q^{\mathrm{oc}} \right)^* \right\rangle = \boldsymbol{\alpha}^H \mathbf{A}_{pq} \boldsymbol{\alpha} \qquad (9)$$

where $\langle \cdot \rangle$ denotes the time average, and where

$$\mathbf{A}_{pq} = \iint_{S_\infty} \frac{e^{j\boldsymbol{k}\cdot[\boldsymbol{r}_q - \boldsymbol{r}_p]}}{\omega^2 \mu_0^2} \mathbf{G}^H(\Omega) \left\langle \boldsymbol{E}^{\mathrm{i}}(\Omega) \left(\boldsymbol{E}^{\mathrm{i}}(\Omega) \right)^H \right\rangle \mathbf{G}(\Omega) \mathrm{d}\Omega \qquad (10)$$

has been generalized to the distributed sky source $\langle \boldsymbol{E}^{\mathrm{i}}(\Omega)(\boldsymbol{E}^{\mathrm{i}}(\Omega))^H \rangle$, which is a matrix of power densities in steradians. This matrix is called the coherency matrix of the source, which is assumed to be known. Note that (10) reduces to (8) in the noiseless case and for point sources (i.e., Dirac distribution functions for the source directions).

A special case occurs for unpolarized sources [9], [10]. Then, the source coherency matrix becomes diagonal, i.e., $\langle E_\theta^{\mathrm{i}}(E_\phi^{\mathrm{i}})^* \rangle = \langle E_\phi^{\mathrm{i}}(E_\theta^{\mathrm{i}})^* \rangle = 0$ and $\langle |E_\theta^{\mathrm{i}}|^2 \rangle = \langle |E_\theta^{\mathrm{i}}|^2 \rangle = P^{\mathrm{i}}(\Omega)/2$, where $P^{\mathrm{i}}(\Omega)$ is the spectral power of the incident field. The unpolarized field can be viewed as radiated by a black

---

[2]Alternatively, one can also choose to consider two orthogonally-polarized reference sources in the same direction.

body at an equivalent noise temperature $T_{\mathrm{sky}}(\Omega)$. Hence, when using the Rayleigh-Jeans approximation of Planck's law, we have that $P^{\mathrm{i}}(\Omega) = 4k_{\mathrm{B}} T_{\mathrm{sky}}(\Omega) Z_0 f^2 / c_0^2$, where f is frequency, c_0 is the speed of light in vacuum, and Z_0 is the impedance of free-space. For unpolarized sources, (10) therefore reduces to

$$\mathbf{A}_{pq} = \frac{k_{\mathrm{B}}}{2\pi^2 Z_0} \iint\limits_{S_\infty} T_{\mathrm{sky}}(\Omega) \mathbf{G}^H \mathbf{G} e^{j\boldsymbol{k}\cdot[\boldsymbol{r}_q - \boldsymbol{r}_p]} \mathrm{d}\Omega \qquad (11)$$

where the $M \times M$ Gramian matrix $\mathbf{G}^H \mathbf{G}$ of the basis function patterns needs to be determined only once.

It is important to note that $\mathbf{G}^H \mathbf{G} = \mathbf{G}^H \mathbf{U}^H \mathbf{U} \mathbf{G}$, where $\mathbf{U}$ is a unitary matrix. Hence, applying a unitary transformation to an unpolarized source field yields an identical matrix block $\mathbf{A}_{pq}$. This unitary ambiguity [11] may here lead to an ambiguous way of determining the pattern expansion coefficients. To resolve this ambiguity, one needs to perform additional measurements on (artificial) polarized sources. Also, since we assume all EEPs to be equal, the open circuit voltage response of the elements will be the same except for the phase shift. In the correlation process the voltage response of one element is multiplied by the conjugated voltage response of another element, which implies that the phase of the common EEP cancels and hence becomes unidentifiable [7, Ch. 5]. This may cause an ambiguity in the solutions for the complex-valued CBFP coefficients $\{\alpha_m\}$. This ambiguity vanishes for real-valued coefficients. Our numerical simulations show that the use of real-valued coefficients already provides percent level accuracy.

IV. DETERMINATION OF PATTERN EXPANSION COEFFICIENTS

Following the above approach, the open-circuit voltage covariance matrix $\mathbf{R}^{\mathrm{oc}}$ is modeled as

$$\mathbf{R}^{\mathrm{oc}} = \begin{bmatrix} \boldsymbol{\alpha}^H \mathbf{A}_{11} \boldsymbol{\alpha} & \cdots & \boldsymbol{\alpha}^H \mathbf{A}_{1N} \boldsymbol{\alpha} \\ \vdots & \ddots & \vdots \\ \boldsymbol{\alpha}^H \mathbf{A}_{N1} \boldsymbol{\alpha} & \cdots & \boldsymbol{\alpha}^H \mathbf{A}_{NN} \boldsymbol{\alpha} \end{bmatrix} \qquad (12)$$

which can be least-squares-fit to the measured open-circuited voltage covariance matrix $\mathbf{R}^{\mathrm{oc,m}}$ to find $\boldsymbol{\alpha}$. However, if only the matched-terminated voltage covariance matrix $\mathbf{R}^{\mathrm{m}}$ is available, one can use the transformation

$$\mathbf{R}^{\mathrm{oc,m}} = \mathbf{L}^{-1} \mathbf{R}^{\mathrm{m}} \mathbf{L}^{-H} \qquad (13)$$

where $\mathbf{L} = \sqrt{Z_{0,\mathrm{ref}}} (\mathbf{Z} + Z_{0,\mathrm{ref}} \mathbf{I})^{-1}$, and where $Z_{0,\mathrm{ref}}$ is the terminated load impedance, $\mathbf{Z}$ is the (modeled or measured) input impedance matrix of the receiver (or antenna) outputs, and $\mathbf{I}$ is the identity matrix.

The difference matrix $\mathbf{R}^{\mathrm{oc,d}}$ between the measured and modeled open-circuit voltage covariance matrix is computed as

$$\begin{aligned} \mathbf{R}^{\mathrm{oc,d}} &= \mathbf{R}^{\mathrm{oc,m}} - \mathbf{R}^{\mathrm{oc}} \\ &= \begin{bmatrix} R_{11}^{\mathrm{oc,m}} & \cdots & R_{1N}^{\mathrm{oc,m}} \\ \vdots & \ddots & \vdots \\ R_{N1}^{\mathrm{oc,m}} & \cdots & R_{NN}^{\mathrm{oc,m}} \end{bmatrix} \\ &\quad - \begin{bmatrix} \boldsymbol{\alpha}^H \mathbf{A}_{11} \boldsymbol{\alpha} & \cdots & \boldsymbol{\alpha}^H \mathbf{A}_{1N} \boldsymbol{\alpha} \\ \vdots & \ddots & \vdots \\ \boldsymbol{\alpha}^H \mathbf{A}_{N1} \boldsymbol{\alpha} & \cdots & \boldsymbol{\alpha}^H \mathbf{A}_{NN} \boldsymbol{\alpha} \end{bmatrix} \end{aligned} \qquad (14)$$
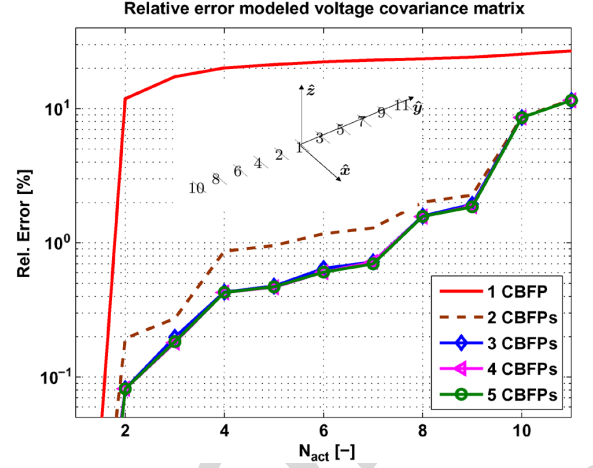

Fig. 1. Relative least-squares fitting error ϵ of the modeled voltage output covariance matrix $\mathbf{R}^{\mathrm{oc}}$ [cf. (15)] as a function of the number of antenna outputs used for fitting. Results are for the 11-element dipole array and for various numbers of CBFPs.

so that $\boldsymbol{\alpha}$ can be found by minimizing the relative error (ratio of Frobenius norms)

$$\epsilon = \arg\min_{\boldsymbol{\alpha}} \left\{ \sqrt{ \frac{\sum_{p,q} |R_{pq}^{\mathrm{oc,m}} - \boldsymbol{\alpha}^H \mathbf{A}_{pq} \boldsymbol{\alpha}|^2}{\sum_{p,q} |R_{pq}^{\mathrm{oc,m}}|^2} } \right\}. \qquad (15)$$

where the number of incoherent point sources r [cf. (8)] must be larger or equal to the number of basis functions M to obtain a unique solution for $\boldsymbol{\alpha}$.

V. NUMERICAL RESULTS

To demonstrate the capabilities of the proposed method, we have considered two examples of relatively small one-dimensional phased-arrays of 11 antenna elements that have been modeled using the numerical method described in [12]. The first example is an array of x-oriented half wavelength dipoles having an inter-element spacing of $\lambda_0/2$ that are positioned along the y-axis, and $\lambda_0/4$ meters above an infinite ground plane (see Fig. 1). Each dipole has a strip width of 1 mm. The second example represents a more complex and strongly coupled array of interconnected tapered-slot antennas (TSAs, see Fig. 2) whose geometrical dimensions are similar to those described in [13], albeit with an element separation distance of $0.38\lambda_0$. The antennas are illuminated by five x-polarized reference plane wave fields incident from $\theta = \{10°, 20°, 30°, 40°, 50°\}$, which give rise to a rank-five voltage covariance matrix. In practice, however, the array patterns (and thus the covariance matrix) will be slightly different from the ideal (simulated) ones. To emulate this difference, we have perturbed the simulated patterns by replacing the open-circuited EEPs by the short-circuited ones. This yields a covariance matrix which we then attempt to model through open-circuited CBFPs.

Figs. 1 and 2 show the relative least-squares fitting error [cf. (15)] of the modeled voltage covariance matrix for the 11-element dipole and TSA arrays, respectively. For this purpose, we have used Matlab's "fminsearch" optimization function with the initial estimate $\boldsymbol{\alpha} = C[1, 0, \ldots, 0]^T$, since the first basis
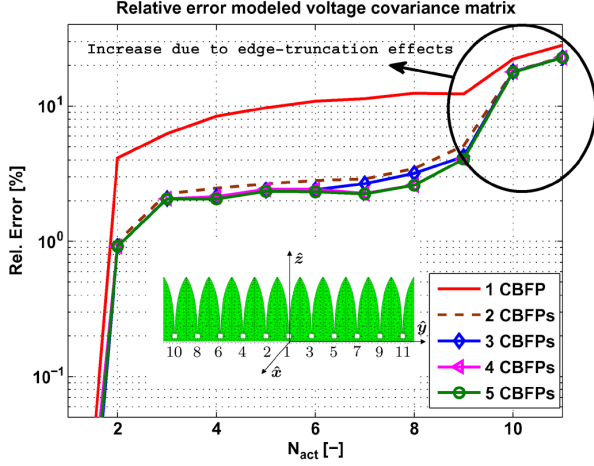
Fig. 2. Relative least-squares fitting error ϵ of the modeled voltage output co-variance matrix $\mathbf{R}^{\mathrm{oc}}$ [cf. (15)] as a function of the number of antenna outputs used for fitting. Results are for the 11-element tapered slot antenna array and for various numbers of CBFPs.
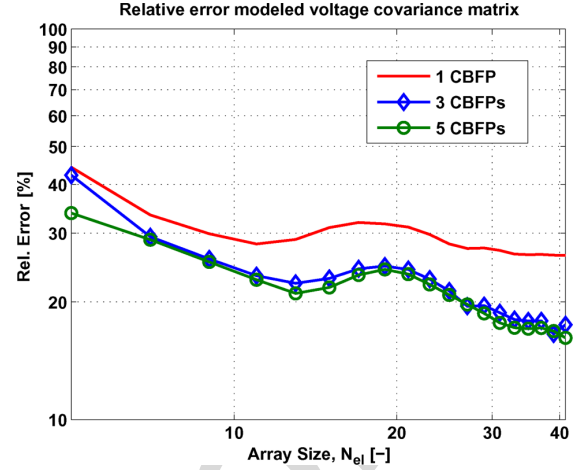

Fig. 3. Relative least-squares fitting error ϵ of the modeled output covariance matrix $\mathbf{R}^{\mathrm{oc}}$ [cf. (15)] as a function of the tapered slot antenna array size (i.e., the number of antenna elements, N_{el}). All outputs are used for fitting, and the results are shown for various numbers of CBFPs.

function is expected to be dominant in modeling the EEP. The scaling constant C is chosen to approximately match the gain in the observations. This initial choice also ensures that the mini-mization yields a physically meaningful result. Furthermore, to ease the minimization, we searched for real-valued expansion coefficients only, which already give sufficiently accurate re-sults as indicated by Figs. 1 and 2.

The method does work for complex-valued expansion coef-ficients, however, there exists a phase ambiguity for the case of incoherent reference sources. For instance, for θ-polarized ref-erence sources, the 2×2 source coherency matrix $\boldsymbol{E}^{\mathrm{i}}(\boldsymbol{E}^{\mathrm{i}})^{H}$ in (8) has only one real-valued element corresponding to the power of the incident source field. Because we measure the powers of incoherent source fields, one can calibrate for the amplitude of the beam pattern only, even though the relative phase dif-ference between the antenna output signals can be modeled for each received source field. The phase variation of each EEP fol-lows from the summed basis function patterns, however, not in an unambiguous manner if one solves for complex-valued expansion coefficients for incoherent source fields. The phase ambiguity disappears by choosing real-valued expansion coef-ficients, so that the relative phase difference between the basis function patterns for each element is fixed and set to zero. Lim-iting to real-valued expansion coefficients means that one can compensate for matching errors pertaining to real-valued ter-minations only. An open question therefore is: how can this phase degeneracy can be broken? One possible solution that has been proposed is to measure on a few additional artificial refer-ence sources whose incident field is given in both amplitude and phase.

To demonstrate the effect of including edge elements in the error minimization, the fitting is performed for a limited number of receiver outputs, i.e., for an $N_{\mathrm{act}} \times N_{\mathrm{act}}$ covariance matrix block. The fitting error is therefore shown as a function of N_{act}. Furthermore, this error is shown for various numbers of CBFPs. It turns out that, as few as 3 CBFPs are needed to predict the an-tenna covariance matrix down to an error of about 2–3%. How-ever, the results also demonstrate that, if $N_{\mathrm{act}} \to N$, i.e., if

edge-element are included in the fitting, the basic assumption that all EEPs are identical ceases to hold. This is manifested by the rapid increase in the fitting error for $N_{\mathrm{act}} > 8$, particularly for the strongly-coupled TSAs in Fig. 2. Hence, and as expected, the accuracy increases for larger arrays (smaller edge-truncation effects). A further improvement may be possible by different optimization algorithms which specifically solve for the struc-ture in (15) (possibly semi-analytical), or by more general par-ticle swarm optimizers (see e.g. [14], [15]).

Fig. 3 confirms the above hypothesis that, as the array size increases (larger N_{el}), the fitting error of the output covariance matrix generally decreases. This can be understood by realizing that the proposed method is entirely founded on the assumption that all embedded element patterns are identical. Indeed, our method essentially implies that the array beam can be modeled by an array factor multiplied by a single unknown embedded element pattern which is expanded in terms of a few relatively slowly varying CBFPs. Note, however, that the error ϵ does not decrease monotonically as N_{el} increases, which may be caused by the mechanism of field interference across the face of the array which differs for different array sizes (array truncation effects). Furthermore, and in accordance with Figs. 1 and 2, one can observe that the fitting error decreases if more CBFPs are employed.

Fig. 4(a) and (b) show the actual and resulting modeled power far-field patterns when the array beam is scanned to $\theta = 30°$. In addition, the relative local gain difference (RLGD) is shown for both the 11-element dipole and TSA arrays. The RLGD is computed as the absolute local gain difference relative to the global maximum gain. The modeled beams pertain to the cases where a single (primary) CBFP and the larger sets of 3 and 5 CBFPs are employed. It is observed that by employing only 3 CBFPs, the RLGD reaches a level which is smaller than -40 dB for the dipole array, and -30 dB for the TSA array, over the entire range of observation angles. Increasing the number of secondary CBFPs does not lead to an improved accuracy, be-cause we have reached the point beyond which the EEPs cannot be regarded identical anymore. This effect is more pronounced
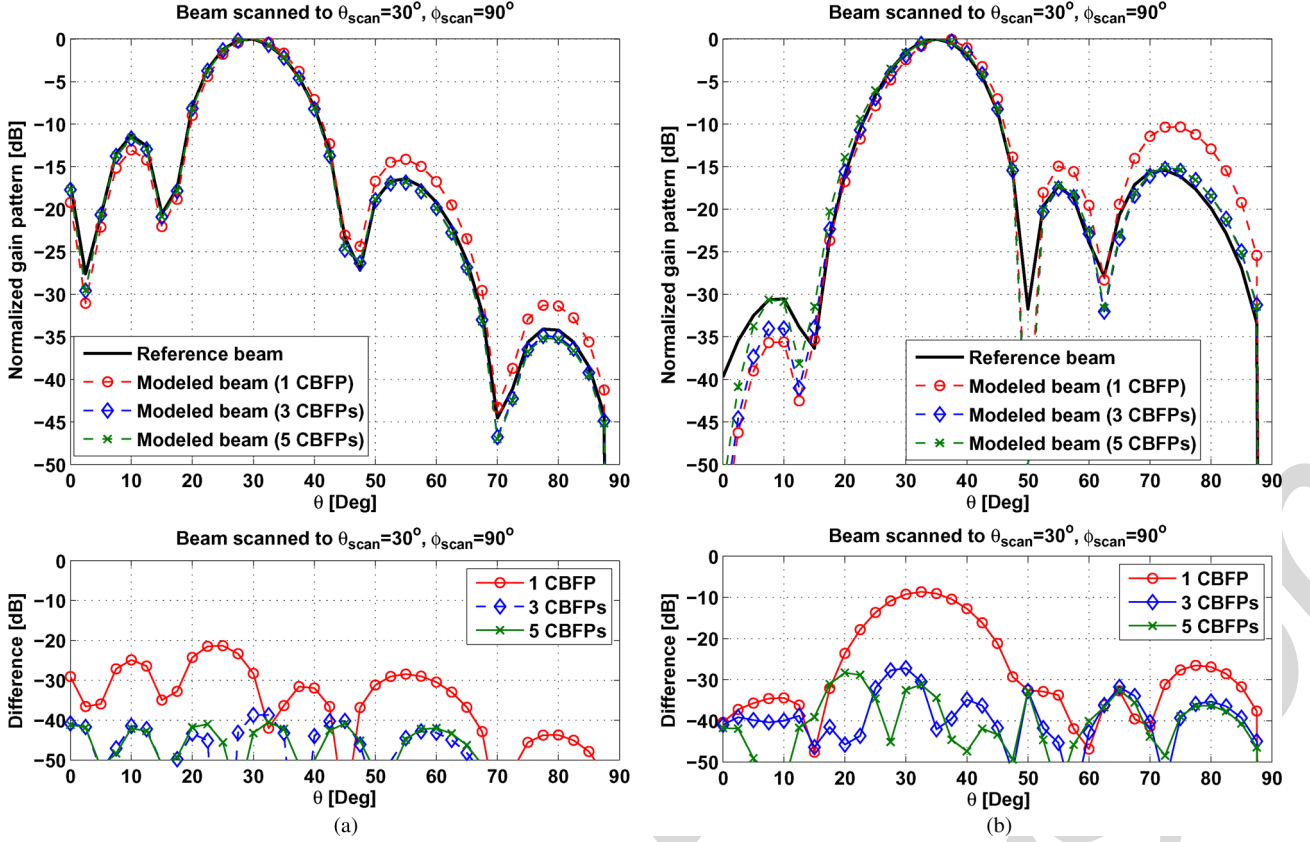
Fig. 4. Reference and modeled normalized array power gain patterns for various numbers of employed CBFPs, for (a) the 11-element dipole antenna array (30° scan in the H-plane); (b) the 11-element tapered slot antenna array (30° scan in the E-plane). The power gain pattern difference is computed relative to the maximum pattern gain.

for the TSA array, which support our conclusions on the validity of the proposed method. Another interesting observation is that the beam-pointing error has been correctly predicted in Fig. 4. At this point, one can adjust the weights to compensate for this error (calibration).

VI. SOLUTION STABILITY

It is important to examine the solution stability of the expansion coefficient vector $\boldsymbol{\alpha}$ as a function of the location of the sky reference sources for a given set of basis function patterns (CBFPs). Toward this end, we recall the analogous situation that, in a method-of-moment approach, the unknown current is expanded in M known basis functions and the integral equation is tested M times to yield a matrix equation which can be solved for the unknown expansion coefficient vector. The matrix condition number is then a measure for the solution stability, which depends on the chosen basis and test functions [4, pp. 41–44]. Note the similarity with the herein proposed method, where each radiation pattern (EEP) is expanded in terms of M CBFPs and where the (least-squares) residual pattern error is measured (tested) in several different directions using $r \geq M$ point sources in the sky (point matching). Also, and as opposed to solving a linear matrix equation as in conventional MoM approaches, the unknown expansion coefficient vector $\boldsymbol{\alpha}$ is determined by solving the non-linear covariance-matrix-fitting problem (15) whose solution is not known in closed form.

For the present stability analysis, we therefore reduce the non-linear fitting problem (of complex correlator output powers) to a linear one (of complex antenna output voltages) and assess the solution stability of $\boldsymbol{\alpha}$ through the matrix condition number. The penalty for not fitting at once to a rank r covariance matrix for r incoherent perfectly-polarized sources (as done above), is that we must now measure the antenna output voltage vector for each source at a time. Nonetheless, the qualitative observations/conclusions for the actual non-linear fitting problem in (15) are believed to be similar to the linear fitting problem insofar the effect of the position of sky reference sources on the solution stability is concerned.

Consider a hypothetical infinite array of radiators placed a distance $\lambda_0/2$ apart along the y-axis (similar to Fig. 1), each having the same $\cos(\theta)$-type of EEP. The r incoherent sky reference sources are x-polarized and located in the $\phi = \pi/2$ plane at $\theta = \{\Delta\theta, 2\Delta\theta, \ldots, M\Delta\theta\}$. In addition, a total of $M \leq r$ CBFPs are employed for the EEP, whose set is found through (4), i.e.,

$$\{g_{x;m}\}_{m=1}^{M} = \left\{\cos(\theta)e^{j\pi\left(\frac{M+1}{2} - m\right)\sin(\theta)}\right\}_{m=1}^{M} \quad (16)$$

for $M \in \{3, 5, 7, \ldots\}$ and $\phi = \pi/2$. Note that $g_x = \cos(\theta)$ for $M = 1$.

In the receiving situation (cf. Section III), the pth open-circuited port voltage is defined as $V_p^{\text{oc}} = (j\omega\mu_0)^{-1}\boldsymbol{f}_p(\Omega_m) \cdot \boldsymbol{E}^{\text{i}}(\Omega_m)$, where $\boldsymbol{f}_p = \sum_{m=1}^{M}\alpha_m g_{x;m}(\theta_m)\hat{\boldsymbol{x}}$ is the modeled
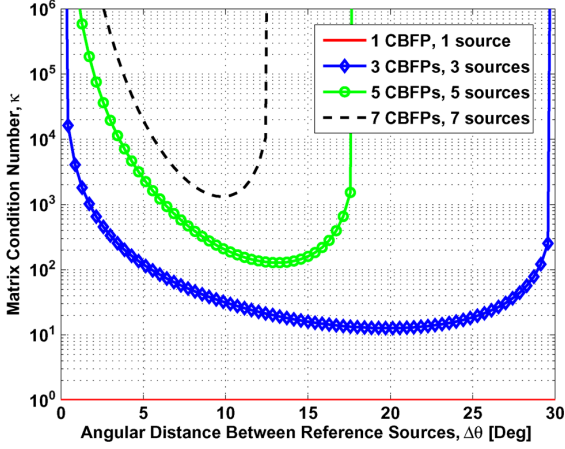
Fig. 5. Matrix condition number κ of the matrix $\mathbf{A}$ for determining the expansion coefficient vector $\boldsymbol{\alpha}$ as a function of the number of point sources and their angular separation distance.

transmit pattern of the pth antenna element in the source direction θ_m, and $\boldsymbol{E}^{\mathrm{i}} = \hat{\boldsymbol{x}}$. Next, the r modeled receive voltages for each source direction can be least-squares-fit to the measured ones to obtain the M expansion coefficients. To this end, we solve

$$\mathbf{A}\boldsymbol{\alpha} = \mathbf{V} \tag{17}$$

where the matrix $\mathbf{A}$ is of size $r \times M$ whose elements are given as

$$A_{sm} = (j\omega\mu_0)^{-1} g_{x;m}(\theta_s) \tag{18}$$

for $s = 1, \ldots, r$ and $m = 1, \ldots, M$. The vector $\boldsymbol{\alpha}$ is of size $M \times 1$, and the elements of the measured voltage vector $\mathbf{V}$ of size $r \times 1$ are given as

$$V_s = V_p(\theta_s) \tag{19}$$

which are the output voltages of the pth element, measured consecutively for each source direction. The solution of (17) is given through the Moore-Penrose pseudoinverse [16]

$$\boldsymbol{\alpha} = (\mathbf{A}^H \mathbf{A})^{-1} \mathbf{A}^H \mathbf{V}. \tag{20}$$

In our example, we choose that $M = r$ and we consider the condition number κ of $\mathbf{A}$. Generally, for non-square matrices $\mathbf{A}$, one could consider the ratio of the largest singular value to the smallest one. The condition number normally improves for more sources than basis functions, so we limit ourselves to the case that $M = r$. The results are shown in Fig. 5 for 1, 3, 5, and 7 CBFPs or sources as a function of the source separation distance $\Delta\theta$.

Clearly, for $M > 1$ CBF or source, and as the sky reference sources start to cluster (smaller $\Delta\theta$), the matrix condition number increases. Consequently, the stability of the solution deteriorates which causes the solution accuracy of $\boldsymbol{\alpha}$ to decrease. As a result, the calibration accuracy may decrease rapidly depending upon the system noise level. Generally, the problem is better conditioned for well-separated sources. Furthermore, the matrix condition number improves for fewer sources or CBFPs,

however; the improved solution stability is traded against a decreased solution accuracy if fewer CBFPs are employed (see e.g. Fig. 1). Finally, for the case of M sources or CBFPs, and for $\Delta\theta = 90/M$ degrees, one source is placed exactly in the null of all basis function patterns, $\cos(\theta) = 0$, as a result of which the problem cannot be solved uniquely. Hence, one should prevent to measure sources near pattern nulls for improved stability, particularly if the number of sources is not much larger than the number of CBFPs (i.e., for weakly overdetermined systems).

VII. CONCLUSIONS AND RECOMMENDATIONS

A novel method has been proposed to model the antenna array far-field pattern by a superposition of physics-based basis function patterns, called CBFPs. The expansion coefficients are determined experimentally through a single far-field measurement. In this paper, the proposed expansion method is applied to aperture phased array antennas. If edge-truncation effects are negligible, all embedded element patterns (EEPs) are identical, apart from a phase transformation. Accordingly, CBFPs can be employed for expanding the (average) EEP, while the element positions are incorporated in an array factor. It has been demonstrated for an 11-element array of dipoles and arrays of strongly-coupled tapered slot antennas that only 3 CBFPs are sufficient to achieve a 2–3% least-squares fitting error of the modeled to the reference output voltage covariance matrix. Furthermore, the computed resulting array beam exhibits a local gain error smaller than -30 dB relative to the global gain maximum. The accuracy increases for arrays with smaller edge-truncation effects (larger array size, sparser). We concluded from the stability analysis of the expansion coefficient vector that the clustering of sky reference sources should be avoided and that the location of sources should not coincides with the nulls of the CBFPs, particularly for weakly overdetermined systems.

It has been shown that CBFPs are particularly well suited to model beams that are radiated by antenna arrays. Future research directions include: (i) the generation of separate edge-element CBFPs to further increase the beam modeling accuracy; (ii) the development of dedicated optimization solvers for determining the expansion coefficients; (iii) to apply the proposed method in resolving the unitary matrix ambiguities for unpolarized sources, and; (iv) to extend the method to phased array feeds for reflector antennas, where each CBFP is generated from an aperture source distribution, which results from a primary EEP illuminating the reflector. In the latter case it is natural to represent each CBFP, in turn, by Jacobi and Fourier-Bessel series expansions with fixed expansion coefficients to ease the pattern interpolation.

Finally, we conclude that the proposed technique is potentially capable of speeding up array calibration by one or two orders of magnitude, which is beneficial for applications such as astronomical receivers where antenna radiation characteristics are subject to drifts and must be periodically remeasured to accurately calibrate the instrument.

REFERENCES

[1] H. L. van Trees, *Optimum Array Processing—Part IV of Detection, Estimation, and Modulation Theory*. New York: Wiley, 2002.

[2] M. V. Ivashina, O. Iupikov, R. Maaskant, W. A. van Cappellen, and T. Oosterloo, "An optimal beamforming strategy for wide-field surveys with phased-array-fed reflector antennas," *IEEE Trans. Antennas Propag.*, vol. 59, no. 6, pp. 1864–1875, Jun. 2011.

[3] V. Prakash and R. Mittra, "Characteristic basis function method: A new technique for efficient solution of method of moments matrix equations," *Microw. Opt. Technol.*, vol. 36, pp. 95–100, Jan. 2003.

[4] R. Maaskant, "Analysis of Large Antenna Systems" Ph.D. dissertation, Eindhoven University of Technology, Eindhoven, 2010 [Online]. Available: http://alexandria.tue.nl/extra2/201010409.pdf

[5] W. A. van Cappellen, S. J. Wijnholds, and J. D. Bregman, "Sparse antenna array configurations in large aperture synthesis radio telescopes," in *Proc. 3rd European Radar Conf.*, Manchester, UK, Sep. 2006, pp. 76–79.

[6] S. van der Tol, B. D. Jeffs, and A.-J. van der Veen, "Self-calibration for the LOFAR radio astronomical array," *IEEE Trans. Signal Process.*, vol. 55, no. 9, pp. 4497–4510, Sep. 2007.

[7] S. J. Wijnholds, "Fish-Eye Observing With Phased Array Radio Telescopes," Ph.D. dissertation, Delft University of Technology, Delft, 2010.

[8] Y. Rahmat-Samii and V. Galindo-Israel, "Shaped reflector antenna analysis using the jacobi-bessel series," *IEEE Trans. Antennas Propag.*, vol. 28, no. 4, pp. 425–435, Jul. 1980.

[9] K. F. Warnick, M. V. Ivashina, S. J. Wijnholds, and R. Maaskant, "Polarimetry with phased array antennas: Theoretical framework and definitions," *IEEE Trans. Antennas Propag.*, vol. 60, no. 1, pp. 184–196, Jan. 2012.

[10] R. E. Collin and F. J. Zucker, *Antenna Theory—Part 1*. New York and London: McGraw-Hill, 1969.

[11] J. P. Hamaker, "Understanding radio polarimetry—IV. The full-coherency analogue of scalar self-calibration: Self-alignment, dynamic range and polarimetric fidelity," *Astron. Astrophys. Suppl. Ser.*, vol. 143, no. 3, pp. 515–534, May 2000.

[12] R. Maaskant and B. Yang, "A combined electromagnetic and microwave antenna system simulator for radio astronomy," in *Proc. Eur. Conf. on Antennas and Propag. (EuCAP)*, Nice, France, Nov. 2006, pp. 1–4.

[13] R. Maaskant, M. V. Ivashina, O. Iupikov, E. A. Redkina, S. Kasturi, and D. H. Schaubert, "Analysis of large microstrip-fed tapered slot antenna arrays by combining electrodynamic and quasi-static field models," *IEEE Trans. Antennas Propag.*, vol. 56, no. 6, pp. 1798–1807, Jun. 2011.

[14] S. Wan, P.-J. Chung, and B. Mulgrew, "Near-field array shape calibration," in *Proc. Int. Conf. on Acoustics, Speech, and Signal Processing (ICASSP)*, Prague, Czech Republic, May 2011, pp. 2564–2567.

[15] B. Birge, "PSOT—A particle swarm optimization toolbox for use with Matlab," in *Proc. Swarm Intelligence Symp. (SIS'03)*, Indianapolis, IN, Apr. 2003, pp. 182–186.

[16] E. H. Moore, "On the reciprocal of the general algebraic matrix," *Bull. Amer. Math. Society*, vol. 26, no. 9, pp. 394–395, 1920.

Marianna V. Ivashina (M'11) received the Ph.D. degree in electrical engineering from the Sevastopol National Technical University (SNTU), Ukraine, in 2000.

From 2001 to 2004, she was a Postdoctoral Researcher and, from 2004 to 2010, an Antenna System Scientist at The Netherlands Institute for Radio Astronomy (ASTRON). During this period, she carried out research on an innovative phased array feed (PAF) technology for a new-generation radio telescope, known as the square kilometer array (SKA). The results of these early PAF projects have led to the definition of APERTIF—a PAF system that is being developed at ASTRON to replace the current horn feeds in the Westerbork Synthesis Radio Telescope (WSRT). She was involved in the development of APERTIF during 2008–2010 and acted as an external reviewer at the Preliminary Design Review of the Australian SKA Pathfinder (ASKAP) in 2009. In 2002, she also stayed as a Visiting Scientist with the European Space Agency (ESA), ESTEC, The Netherlands, where she studied multiple-beam array feeds for the satellite telecommunication system large deployable antenna (LDA). She is currently a Senior Scientist at the Department of Earth and Space Sciences (Chalmers University of Technology). Her interests are wideband receiving arrays, antenna system modeling techniques, receiver noise characterization, signal processing for phased arrays, and radio astronomy.

Dr. Ivashina received the URSI Young Scientists Award for the GA URSI, Toronto, Canada (1999), an APS/IEEE Travel Grant, Davos, Switzerland (2000), the 2nd Best Paper Award ("Best Team Contribution") at the ESA Antenna Workshop (2008) and the International Qualification Fellowship of the VINNOVA—Marie Curie Actions Program (2009) and The VR project grant of the Swedish Research Center (2010).

Stefan J. Wijnholds (S'06–M'10) was born in The Netherlands in 1978. He received the M.Sc. degree in astronomy and the M.Eng. degree in applied physics (both *cum laude*) from the University of Groningen, The Netherlands, in 2003, and the Ph.D. degree (*cum laude*) from Delft University of Technology, Delft, The Netherlands, in 2010.

After his graduation in 2003, he joined the R&D Department, ASTRON, the Netherlands Institute for Radio Astronomy, Dwingeloo, where he works with the system design and integration egroup on the development of the next generation of radio telescopes. From 2006 to 2010, he was also affiliated with the Delft University of Technology, Delft. His research interests lie in the area of array signal processing, specifically calibration and imaging, and system design of the next generation of radio telescopes.

Dr. Wijnholds received travel grants for the URSI GASS 2008 in Chicago (Ill.), the Asia-Pacific Radio Science Conference in Toyama, Japan (2010) and the URSI GASS 2011 in Istanbul, Turkey.

Rob Maaskant (M'11) was born in the Netherlands on April, 14, 1978. He received the M.Sc. (*cum laude*) and Ph.D. (*cum laude*) degrees in electrical engineering from the Eindhoven University of Technology, Eindhoven, The Netherlands, in 2003 and 2010, respectively.

From 2003 to 2010, he was employed as an Antenna Research Scientist at the Netherlands Institute of Radio Astronomy (ASTRON). He is currently a Postdoctoral Researcher in the Antenna Group, Chalmers University of Technology, Sweden, for which he won a Rubicon postdoctoral fellowship from the Netherlands Organization for Scientific Research (NWO), 2010. He is the primary author of the CAESAR software; an advanced integral-equation based solver for the analysis of large antenna array systems. His current research interest is in the field of receiving antennas for low-noise applications, meta-material based waveguides, and computational electromagnetics to solve these types of problems.

Dr. Maaskant's Ph.D. was awarded "Best Dissertation of the Electrical Engineering Department, in 2010." He received the 2nd best paper prize ("Best Team Contribution") at the 2008 ESA/ESTEC workshop, Noordwijk, and was awarded a Young Researcher Grant from the Swedish Research Council (VR), in 2011.

Karl F. Warnick (SM'04) received the B.S. degree (*magna cum laude* with University Honors) and the Ph.D. degree from Brigham Young University (BYU), Provo, UT, in 1994 and 1997, respectively.

From 1998 to 2000, he was a Postdoctoral Research Associate and Visiting Assistant Professor in the Center for Computational Electromagnetics, University of Illinois at Urbana-Champaign. Since 2000, he has been a faculty member in the Department of Electrical and Computer Engineering, BYU, where he is currently a Professor. In 2005 and 2007, he was a Visiting Professor at the Technische Universität München, Germany. He has published many scientific articles and conference papers on electromagnetic theory, numerical methods, remote sensing, antenna applications, phased arrays, biomedical devices, and inverse scattering, and is the author of the book *Problem Solving in Electromagnetics, Microwave Circuits, and Antenna Design for Communications Engineering* (Artech House, 2006) and coauthor of *Numerical Analysis for Electromagnetic Integral Equations* (Artech House, 2008) and *Numerical Methods for Engineering: An Introduction Using MATLAB and Computational Electromagnetics Examples* (Scitech, 2010).

Dr. Warnick was a recipient of the National Science Foundation Graduate Research Fellowship, Outstanding Faculty Member award for Electrical and

Computer Engineering (2005), and the BYU Young Scholar Award (2007). He has served the Antennas and Propagation Society as a member of the Education Committee and as a session chair and special session organizer for the International Symposium on Antennas and Propagation and other meetings affiliated with the Society. He is a frequent reviewer for the IEEE TRANSACTIONS ON ANTENNAS AND PROPAGATION and *Antennas and Wireless Propagation Letters*. He has been a member of the Technical Program Committee for the International Symposium on Antennas and Propagation for several years and served as Technical Program Co-Chair for the Symposium in 2007.

Efficient Prediction of Array Element Patterns Using Physics-Based Expansions and a Single Far-Field Measurement

Rob Maaskant, *Member, IEEE,* Marianna V. Ivashina, *Member, IEEE,* Stefan J. Wijnholds, *Member, IEEE,* and Karl F. Warnick, *Senior Member, IEEE*

Abstract—**A method is proposed to predict the antenna array beam through employing a relatively small set of physics-based basis functions—called characteristic basis function patterns (CBFPs)—for modeling the embedded element patterns. The primary CBFP can be measured or extracted from numerical simulations, while additional (secondary) CBFPs are derived from the primary one. Furthermore, each numerically generated CBFP, which is typically simulated/measured for discrete directions only, can in turn be approximated by analytical basis functions with fixed expansion coefficients to evaluate the resulting array pattern at any angle through interpolation. This hierarchical basis reduces the number of unknown expansion coefficients significantly. Accordingly, the CBFP expansion coefficients can be determined through a single far-field measurement of only a few reference sources in the field of view. This is particularly important for multibeam array applications where only a limited number of reference sources are available for predicting the beam shape. Furthermore, this instantaneous beam calibration is fast, i.e., potentially capable to speed up the array calibration by one or two orders of magnitude, which is particularly important if the antenna radiation characteristics are subject to drifts.**

Index Terms—**Beam calibration, far-field pattern, phased array antennas.**

I. INTRODUCTION

IN many antenna array applications it is vitally important to accurately measure the far-field beams as a function of angle, so as to monitor and control the side-lobe level, the beam stability and beam overlap in multibeam applications, to resolve the direction-dependent errors of interferometric imaging arrays, etc. Very fine sampling of the pattern, however, requires a long measurement time during which the system performance

must be time-invariant to prevent the radiation characteristics of high-sensitivity antenna systems from drifting. Consequently, practical beam calibration becomes difficult—if not impossible—if the number of required measurement samples is large. To reduce the beam calibration time, one could measure a number of sky reference sources at once, rather than on a source-by-source basis. More specifically, we will assume that all N antenna element output ports are accessible and that their output voltages are correlated[1] to form an $N \times N$ output covariance matrix $\mathbf{R}$. Although this complicates the beamforming network, $\mathbf{R}$ contains the information of all measured sources via a single measurement. For instance, for r perfectly-polarized incoherent sources in the sky, $\mathbf{R}$ is of rank r, that is, a sum of r rank-one matrices, one for each source. Indeed, a consecutive measurement of r output voltage vectors, one for each source, may be a time-consuming process, particularly if the antenna has to be physically rotated or the sky reference sources have to move to a different location within the field of view (FoV).

Once $\mathbf{R}$ is measured, one can employ antenna array signal processing algorithms to retrieve information about the source(s) [1], which is common practice for interferometric imaging array antennas for radio astronomy [2], MIMO communication, and radar applications. In this paper, however, our objective is to use a known set of incoherent sky reference sources to be able to identify the antenna beam pattern. Note that, even though the presented methodology is general, if only cosmic incoherent power point sources are used, the phase of the pattern cannot be calibrated for, so that we will limit ourselves to modeling the power pattern only. Research is ongoing to eliminate this so-called phase ambiguity by using additional artificial reference sources in the vicinity of the antenna whose radiated fields are known in both amplitude and phase.

Since the number of natural reference sources in the antenna's FoV may be very limited, we will employ a suitable set of complex-valued vector basis function patterns for interpolating the pattern between distant samples. Furthermore, since the basis functions should account for the array element positioning and the intrinsic physics of each radiator, we propose to employ physics-based basis function patterns (e.g. simulated ones, which account for the element geometry and obey Maxwell's equations) to limit the degrees of freedom of the pattern to those that are physically relevant. This generally

leads to a much smaller number of basis functions than a more general mathematical-function-based expansion alone.

It is pointed out that, over the past decade, much attention has been devoted to reducing the number of basis functions for the currents in method-of-moment approaches, so that the matrix equation can be solved in-core on standard desktop computers without compromising the solution accuracy much. These methods have not yet been applied to generate a small set of basis functions for the far-field patterns. Hence, and analogous to the characteristic basis function method for the current (CBFM, [3], [4]), we expand the practical/actual unknown embedded element pattern (EEP) of an antenna array element—thus antenna coupling included—in terms of a few discretely sampled (simulated) characteristic basis function patterns (CBFPs). The first (primary) CBFP is chosen to be the ideal EEP obtained from numerical simulations, which is supposed to be very close to the actual EEP. To further minimize the pattern modeling error, additional (secondary) CBFPs are generated which should be chosen with care as they are expected to compensate certain types of pattern errors. For example; if a manufacturing tolerance in the element geometry is to be expected, it seems natural to simulate the EEP of a few perturbed element geometries and use these as higher-order CBFPs. Hence, the methodology is general but hinges on the way higher-order CBFPs are generated. In this paper, we consider the specific case that the elements are expected to be mismatched. Thus, exciting one element in an array environment causes the output waves to reflect at the mismatched terminations, which in turn excite the elements to contribute to the radiation pattern. Hence, to compensate/model for this pattern change, it seems natural to use the EEPs of the direct neighboring antenna elements as secondary CBFPs and append it to the primary CBFP for the element under consideration. This procedure is repeated for each antenna array element, so that each antenna element supports a set of CBFPs.

Furthermore, the number of pattern expansion coefficients is kept to a minimum by neglecting array truncation effects. As a result, all EEPs are identical (apart from a phase correction) and can therefore be expanded into the same set of CBFPs (apart from a phase correction) with identical expansion coefficients. This is accurate if systematic errors in the EEP are expected for very large regular arrays—dense or sparse—but also for weakly-coupled sparse arrays, or stronger-coupled irregular arrays whenever the synthesized EEP is viewed as an *average* EEP [5]. Note that the pattern change due to mismatch effects is minimal in sparse or weakly-coupled arrays, so that we will consider strongly-coupled antenna arrays only. The methodology allows to use several CBFP expansions for several parts of the array (say central and edge elements) to model differences in EEPs from element to element. However, this would increase the degrees of freedom (number of unknown expansion coefficients) and may lead to non-unique solutions if the number of expansion coefficients becomes too large [6]. Consequently, the sources should move to other places in the field of view to perform additional independent measurements, which is undesired if the beam calibration measurement has to be performed instantaneously in order to prevent drifts in the system performance. For one expansion, only a few CBFP expansion coefficients of

a single (average) array element have to be determined, which requires an equally low amount of incoherent far-field reference sources in the antenna's FoV during the measurement. Accordingly, the expansion coefficients for the pattern are determined indirectly by least-squares fitting the modeled output covariance matrix to the measured one, following similar techniques as in phased array self-calibration [7, Ch. 5].

If desired, and without increasing the number of unknowns, each so-generated CBFP can be represented analytically by a series of mathematical basis functions with fixed expansion coefficients to ease pattern interpolation, such as the Jacobi-Bessel series [8] if the CBFPs are generated by sources distributed over a large aperture, or spherical wave functions if the CBFPs originate from localized source, etc. Expanding a pattern in terms of analytical basis functions is common practice and therefore not discussed further. The herein proposed hierarchical basis therefore expands the numerically-generated CBFPs into many lower-order ones, as opposed to employing a series expansion of analytical functions alone.

The generation of basis function patterns (CBFPs) is discussed in Section II. Afterwards, in Section III, a model is developed for the output covariance matrix, both for perfectly-polarized and unpolarized reference sources. The determination of the pattern expansion coefficients through a least-squares fitting procedure is discussed in Section IV. In Section V, numerical results are presented for an 11-element array of dipoles and strongly coupled tapered-slot antennas whose CBFPs are first extracted from an ideal numerical antenna model, after which these CBFPs are used to model the actual non-ideal array beam, which is herein simulated by summing a perturbed set of embedded element patterns. Finally, in Section VI, the solution stability of the expansion coefficients as a function of the location and distance between the reference point sources is assessed through the matrix condition number.

II. Modeling the Far-Field Beams

It is assumed that the actual/measured unknown E-field EEP of the pth antenna array element, $\boldsymbol{f}_p(\theta, \phi) = E_{\theta;p}(\theta, \phi)\hat{\boldsymbol{\theta}} + E_{\phi;p}(\theta, \phi)\hat{\boldsymbol{\phi}}$, at position $\boldsymbol{r}_p$ can be described by the M_p basis function patterns $\{\boldsymbol{g}_{mp}\}_{m=1}^{M_p}$, i.e.

$$\boldsymbol{f}_p(\theta, \phi) = \sum_{m=1}^{M_p} \alpha_{mp}\boldsymbol{g}_{mp}(\theta, \phi) \tag{1}$$

where $\{\alpha_{mp}\}$ are the M_p unknown complex-valued CBFP expansion coefficients for the pth antenna element. The EEP $\boldsymbol{f}_p$ arises if element p is excited by a current source of unit amplitude while all other terminals are open-circuited. The loaded case is discussed in Section IV.

As stated in the introduction, if edge-truncation effects can be neglected, all EEPs are identical, apart from a phase transformation in accordance to the translated position of the antenna element (array factor), i.e., the qth element pattern is derived from the pth reference one as

$$\boldsymbol{f}_q(\theta, \phi) = \boldsymbol{f}_p(\theta, \phi)e^{-j\boldsymbol{k}(\theta, \phi)\cdot[\boldsymbol{r}_q - \boldsymbol{r}_p]} \tag{2}$$

where the free-space wave vector is herein defined as $\boldsymbol{k}(\theta, \phi) = -(2\pi/\lambda_0)[\sin(\theta)\cos(\phi)\hat{\boldsymbol{x}} + \sin(\theta)\sin(\phi)\hat{\boldsymbol{y}} + \cos(\theta)\hat{\boldsymbol{z}}]$. Note that $[\boldsymbol{r}_q - \boldsymbol{r}_p]$ realizes a phase correction relative to the element p, instead of to the global origin of the array. Accordingly, the qth EEP is expanded as

$$\boldsymbol{f}_q(\theta, \phi) = e^{-j\boldsymbol{k}(\theta,\phi)\cdot[\boldsymbol{r}_q-\boldsymbol{r}_p]} \sum_{m=1}^{M} \alpha_m \boldsymbol{g}_m(\theta, \phi) \qquad (3)$$

for $q = 1, \ldots, N$, where we now have only M CBFP complex-valued expansion coefficients $\{\alpha_m\}$ that need to be determined.

The set of basis function patterns $\{\boldsymbol{g}_m\}$ can be determined on physical grounds. The most dominant basis function $\boldsymbol{g}_1$ (primary CBFP) is the one that is closest to the actual EEP. For this CBFP one can use the simulated (or measured) EEP extracted from a large array environment. The EEP in a real system will only be slightly perturbed from that. If this perturbation is due to slightly mismatched antennas, this change in EEP occurs because of the reflected waves at the antenna terminations that, in turn, excite the nearest antenna neighbors. Our suggestion is therefore to employ the neighboring EEPs as secondary CBFPs to be able to correct for this type of perturbation. As a result, the entire set of CBFPs for a centralized antenna element becomes

$$\{\boldsymbol{g}_m\}_{m=1}^{M} = \left\{ \boldsymbol{g}_1, \boldsymbol{g}_1 e^{-j\boldsymbol{k}(\theta,\phi)\cdot\boldsymbol{d}_1}, \ldots, \boldsymbol{g}_1 e^{-j\boldsymbol{k}(\theta,\phi)\cdot\boldsymbol{d}_M} \right\} \quad (4)$$

where the M nearest EEPs are selected, each of which is derived by applying a phase-pattern correction to $\boldsymbol{g}_1$ in accordance with the geometric offset $\boldsymbol{d}_m$ relative to the element under consideration. It is pointed out that each CBFP can be expanded in terms of a set of analytical basis functions with fixed coefficients to ease pattern interpolation.

In matrix-vector notation, and when dropping the (θ, ϕ) dependence, (3) can be written as

$$\boldsymbol{f}_q = e^{-j\boldsymbol{k}\cdot[\boldsymbol{r}_q-\boldsymbol{r}_p]}\mathbf{G}\boldsymbol{\alpha}, \quad \text{for } q = 1, \ldots, N \qquad (5)$$

where the column-augmented matrix $\mathbf{G} = [\boldsymbol{g}_1, \boldsymbol{g}_2, \cdots, \boldsymbol{g}_M]$ is of size $2 \times M$ (2 far-field components), and the $M \times 1$ column vector $\boldsymbol{\alpha} = [\alpha_1, \alpha_2, \cdots, \alpha_M]^T$, where T denotes the transposition operator. Note that, by assuming $\mathbf{G}$ constant for all array elements, the same relative offset positions of the neighboring antenna elements is assumed, which may not be true for edge elements, but this is a consequence of assuming that all EEPs are identical.

Eq. (5) provides a mathematical model for all EEPs, where $\boldsymbol{\alpha}$ is the only unknown vector that needs to be determined, which can be done through performing a single far-field measurement. More specifically, for a sky containing a number of relatively strong and incoherent far-field sources in the FoV, one commonly measures a voltage covariance matrix at the receiver outputs. Our approach is therefore to least-squares-fit the $N \times N$ modeled covariance matrix to the measured one in order to find $\boldsymbol{\alpha}$ as discussed below.

III. Modeling the Voltage Covariance Matrix

A. Far-Field Point Sources (No Noise)

The open-circuited pth output port voltage, which arises due to a deterministic perfectly-polarized plane-wave field $\boldsymbol{E}^{\text{i}}(\Omega)$ incident from direction Ω, can be computed through antenna reciprocity as: $V_p^{\text{oc}} = (1/j\omega\mu_0)\boldsymbol{f}_p(\Omega) \cdot \boldsymbol{E}^{\text{i}}(\Omega)$ [4, p. 27]. Upon neglecting estimation error, the element R_{pq}^{oc} of the $N \times N$ output voltage covariance matrix $\mathbf{R}^{\text{oc}}$ is thus computed as

$$R_{pq}^{\text{oc}} = \left\langle V_p^{\text{oc}} \left(V_q^{\text{oc}}\right)^* \right\rangle = \frac{\left[\boldsymbol{f}_p(\Omega) \cdot \boldsymbol{E}^{\text{i}}(\Omega)\right] \left[\boldsymbol{f}_q(\Omega) \cdot \boldsymbol{E}^{\text{i}}(\Omega)\right]^*}{\omega^2 \mu_0^2} \qquad (6)$$

where $*$ indicates conjugation. Substituting (5) in (6), yields

$$\begin{aligned} R_{pq}^{\text{oc}} &= \frac{e^{j\boldsymbol{k}\cdot[\boldsymbol{r}_q-\boldsymbol{r}_p]}}{\omega^2\mu_0^2} \left[(\mathbf{G}\boldsymbol{\alpha}) \cdot \boldsymbol{E}^{\text{i}}\right] \left[(\mathbf{G}\boldsymbol{\alpha}) \cdot \boldsymbol{E}^{\text{i}}\right]^* \\ &= \boldsymbol{\alpha}^H \left[\frac{e^{j\boldsymbol{k}\cdot[\boldsymbol{r}_q-\boldsymbol{r}_p]}}{\omega^2\mu_0^2} \mathbf{G}^H \boldsymbol{E}^{\text{i}}(\boldsymbol{E}^{\text{i}})^H \mathbf{G}\right] \boldsymbol{\alpha} \\ &= \boldsymbol{\alpha}^H \mathbf{A}_{pq} \boldsymbol{\alpha} \end{aligned} \qquad (7)$$

where the matrix block $\mathbf{A}_{pq}$ is of size $M \times M$ and given as

$$\mathbf{A}_{pq} = \sum_{s=1}^{r} \frac{e^{j\boldsymbol{k}\cdot[\boldsymbol{r}_q-\boldsymbol{r}_p]}}{\omega^2\mu_0^2} \mathbf{G}^H(\Omega_s)\boldsymbol{E}^{\text{i}}(\Omega_s)\left(\boldsymbol{E}^{\text{i}}(\Omega_s)\right)^H \mathbf{G}(\Omega_s) \qquad (8)$$

for r incoherent reference sources observed at the r distinct directions[2] $\Omega_1, \ldots, \Omega_r$. Note that the matrix block $\mathbf{A}_{pq}$ can be readily computed, since the basis functions and reference sources are supposed to be known. The problem is therefore to find $\boldsymbol{\alpha}$ in (7) so that R_{pq}^{oc} is modeled best in a least-squares sense $\forall p, q \in \{1, \ldots, N\}$.

B. Distributed Far-Field Sources (Noise Present)

In the more general case of distributed sources, and in the presence of noise, the statistical expectation $\mathbb{E}\{V_p^{\text{oc}}(V_q^{\text{oc}})^*\}$ of each voltage covariance matrix element must be estimated. Assuming that the statistical noise sources are (wide-sense) stationary random processes which exhibit ergodicity, ensemble averages may be replaced by a time average of a sufficiently long sample (realization) of the process to minimize estimation error. Hence,

$$\mathbb{E}\left\{R_{pq}^{\text{oc}}\right\} = \left\langle V_p^{\text{oc}} \left(V_q^{\text{oc}}\right)^* \right\rangle = \boldsymbol{\alpha}^H \mathbf{A}_{pq} \boldsymbol{\alpha} \qquad (9)$$

where $\langle \cdot \rangle$ denotes the time average, and where

$$\mathbf{A}_{pq} = \iint\limits_{S_\infty} \frac{e^{j\boldsymbol{k}\cdot[\boldsymbol{r}_q-\boldsymbol{r}_p]}}{\omega^2\mu_0^2} \mathbf{G}^H(\Omega) \left\langle \boldsymbol{E}^{\text{i}}(\Omega) \left(\boldsymbol{E}^{\text{i}}(\Omega)\right)^H \right\rangle \mathbf{G}(\Omega)\mathrm{d}\Omega \qquad (10)$$

has been generalized to the distributed sky source $\langle \boldsymbol{E}^{\text{i}}(\Omega)(\boldsymbol{E}^{\text{i}}(\Omega))^H \rangle$, which is a matrix of power densities in steradians. This matrix is called the coherency matrix of the source, which is assumed to be known. Note that (10) reduces to (8) in the noiseless case and for point sources (i.e., Dirac distribution functions for the source directions).

A special case occurs for unpolarized sources [9], [10]. Then, the source coherency matrix becomes diagonal, i.e., $\langle E_\theta^{\text{i}}(E_\phi^{\text{i}})^* \rangle = \langle E_\phi^{\text{i}}(E_\theta^{\text{i}})^* \rangle = 0$ and $\langle |E_\theta^{\text{i}}|^2 \rangle = \langle |E_\theta^{\text{i}}|^2 \rangle = P^{\text{i}}(\Omega)/2$, where $P^{\text{i}}(\Omega)$ is the spectral power of the incident field. The unpolarized field can be viewed as radiated by a black

---

[2]Alternatively, one can also choose to consider two orthogonally-polarized reference sources in the same direction.

body at an equivalent noise temperature $T_{\text{sky}}(\Omega)$. Hence, when using the Rayleigh-Jeans approximation of Planck's law, we have that $P^{\text{i}}(\Omega) = 4k_{\text{B}}T_{\text{sky}}(\Omega)Z_0 f^2/c_0^2$, where f is frequency, c_0 is the speed of light in vacuum, and Z_0 is the impedance of free-space. For unpolarized sources, (10) therefore reduces to

$$\mathbf{A}_{pq} = \frac{k_{\text{B}}}{2\pi^2 Z_0} \iint\limits_{S_\infty} T_{\text{sky}}(\Omega)\mathbf{G}^H\mathbf{G}e^{j\boldsymbol{k}\cdot[\boldsymbol{r}_q - \boldsymbol{r}_p]}\mathrm{d}\Omega \qquad (11)$$

where the $M \times M$ Gramian matrix $\mathbf{G}^H\mathbf{G}$ of the basis function patterns needs to be determined only once.

It is important to note that $\mathbf{G}^H\mathbf{G} = \mathbf{G}^H\mathbf{U}^H\mathbf{U}\mathbf{G}$, where $\mathbf{U}$ is a unitary matrix. Hence, applying a unitary transformation to an unpolarized source field yields an identical matrix block $\mathbf{A}_{pq}$. This unitary ambiguity [11] may here lead to an ambiguous way of determining the pattern expansion coefficients. To resolve this ambiguity, one needs to perform additional measurements on (artificial) polarized sources. Also, since we assume all EEPs to be equal, the open circuit voltage response of the elements will be the same except for the phase shift. In the correlation process the voltage response of one element is multiplied by the conjugated voltage response of another element, which implies that the phase of the common EEP cancels and hence becomes unidentifiable [7, Ch. 5]. This may cause an ambiguity in the solutions for the complex-valued CBFP coefficients $\{\alpha_m\}$. This ambiguity vanishes for real-valued coefficients. Our numerical simulations show that the use of real-valued coefficients already provides percent level accuracy.

IV. DETERMINATION OF PATTERN EXPANSION COEFFICIENTS

Following the above approach, the open-circuit voltage co-variance matrix $\mathbf{R}^{\text{oc}}$ is modeled as

$$\mathbf{R}^{\text{oc}} = \begin{bmatrix} \boldsymbol{\alpha}^H\mathbf{A}_{11}\boldsymbol{\alpha} & \cdots & \boldsymbol{\alpha}^H\mathbf{A}_{1N}\boldsymbol{\alpha} \\ \vdots & \ddots & \vdots \\ \boldsymbol{\alpha}^H\mathbf{A}_{N1}\boldsymbol{\alpha} & \cdots & \boldsymbol{\alpha}^H\mathbf{A}_{NN}\boldsymbol{\alpha} \end{bmatrix} \qquad (12)$$

which can be least-squares-fit to the measured open-circuited voltage covariance matrix $\mathbf{R}^{\text{oc,m}}$ to find $\boldsymbol{\alpha}$. However, if only the matched-terminated voltage covariance matrix $\mathbf{R}^{\text{m}}$ is available, one can use the transformation

$$\mathbf{R}^{\text{oc,m}} = \mathbf{L}^{-1}\mathbf{R}^{\text{m}}\mathbf{L}^{-H} \qquad (13)$$

where $\mathbf{L} = \sqrt{Z_{0,\text{ref}}}(\mathbf{Z} + Z_{0,\text{ref}}\mathbf{I})^{-1}$, and where $Z_{0,\text{ref}}$ is the ter-minated load impedance, $\mathbf{Z}$ is the (modeled or measured) input impedance matrix of the receiver (or antenna) outputs, and $\mathbf{I}$ is the identity matrix.

The difference matrix $\mathbf{R}^{\text{oc,d}}$ between the measured and mod-eled open-circuit voltage covariance matrix is computed as

$$\begin{aligned} \mathbf{R}^{\text{oc,d}} &= \mathbf{R}^{\text{oc,m}} - \mathbf{R}^{\text{oc}} \\ &= \begin{bmatrix} R_{11}^{\text{oc,m}} & \cdots & R_{1N}^{\text{oc,m}} \\ \vdots & \ddots & \vdots \\ R_{N1}^{\text{oc,m}} & \cdots & R_{NN}^{\text{oc,m}} \end{bmatrix} \\ &- \begin{bmatrix} \boldsymbol{\alpha}^H\mathbf{A}_{11}\boldsymbol{\alpha} & \cdots & \boldsymbol{\alpha}^H\mathbf{A}_{1N}\boldsymbol{\alpha} \\ \vdots & \ddots & \vdots \\ \boldsymbol{\alpha}^H\mathbf{A}_{N1}\boldsymbol{\alpha} & \cdots & \boldsymbol{\alpha}^H\mathbf{A}_{NN}\boldsymbol{\alpha} \end{bmatrix} \end{aligned} \qquad (14)$$
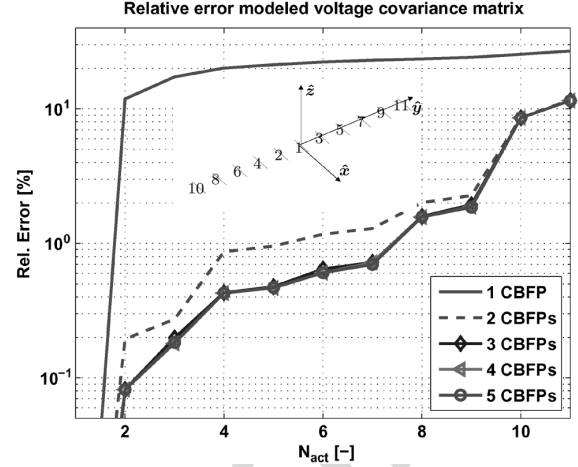

Fig. 1. Relative least-squares fitting error ϵ of the modeled voltage output co-variance matrix $\mathbf{R}^{\text{oc}}$ [cf. (15)] as a function of the number of antenna outputs used for fitting. Results are for the 11-element dipole array and for various num-bers of CBFPs.

so that $\boldsymbol{\alpha}$ can be found by minimizing the relative error (ratio of Frobenius norms)

$$\epsilon = \arg\min_{\boldsymbol{\alpha}} \left\{ \sqrt{\frac{\sum\limits_{p,q} |R_{pq}^{\text{oc,m}} - \boldsymbol{\alpha}^H\mathbf{A}_{pq}\boldsymbol{\alpha}|^2}{\sum\limits_{p,q} |R_{pq}^{\text{oc,m}}|^2}} \right\}. \qquad (15)$$

where the number of incoherent point sources r [cf. (8)] must be larger or equal to the number of basis functions M to obtain a unique solution for $\boldsymbol{\alpha}$.

V. NUMERICAL RESULTS

To demonstrate the capabilities of the proposed method, we have considered two examples of relatively small one-dimen-sional phased-arrays of 11 antenna elements that have been modeled using the numerical method described in [12]. The first example is an array of x-oriented half wavelength dipoles having an inter-element spacing of $\lambda_0/2$ that are positioned along the y-axis, and $\lambda_0/4$ meters above an infinite ground plane (see Fig. 1). Each dipole has a strip width of 1 mm. The second example represents a more complex and strongly coupled array of interconnected tapered-slot antennas (TSAs, see Fig. 2) whose geometrical dimensions are similar to those described in [13], albeit with an element separation distance of $0.38\lambda_0$. The antennas are illuminated by five x-polarized reference plane wave fields incident from $\theta = \{10°, 20°, 30°, 40°, 50°\}$, which give rise to a rank-five voltage covariance matrix. In practice, however, the array patterns (and thus the covariance matrix) will be slightly different from the ideal (simulated) ones. To emulate this difference, we have perturbed the sim-ulated patterns by replacing the open-circuited EEPs by the short-circuited ones. This yields a covariance matrix which we then attempt to model through open-circuited CBFPs.

Figs. 1 and 2 show the relative least-squares fitting error [cf. (15)] of the modeled voltage covariance matrix for the 11-el-ement dipole and TSA arrays, respectively. For this purpose, we have used Matlab's "fminsearch" optimization function with the initial estimate $\boldsymbol{\alpha} = C[1, 0, \ldots, 0]^T$, since the first basis
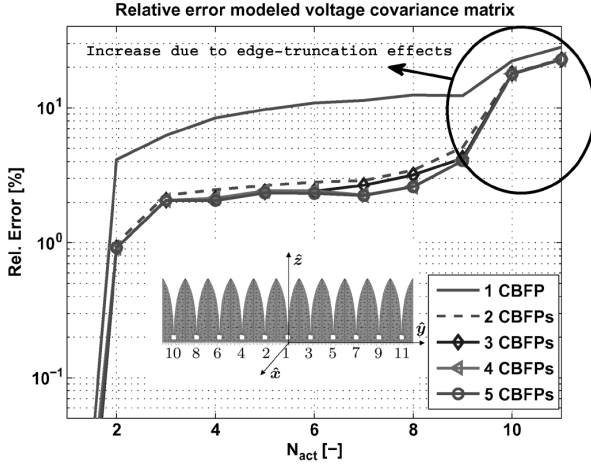
Fig. 2. Relative least-squares fitting error ϵ of the modeled voltage output co-variance matrix $\mathbf{R}^{oc}$ [cf. (15)] as a function of the number of antenna outputs used for fitting. Results are for the 11-element tapered slot antenna array and for various numbers of CBFPs.
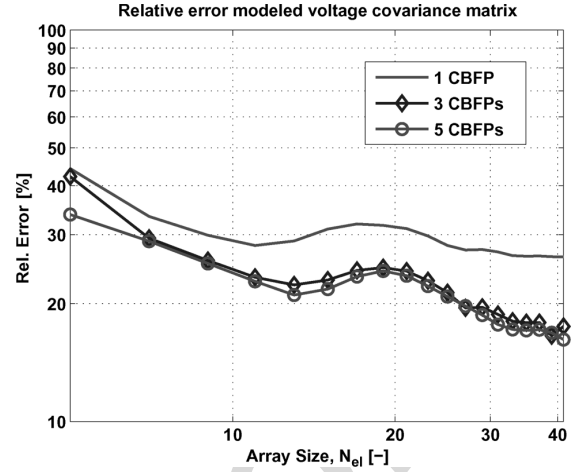

Fig. 3. Relative least-squares fitting error ϵ of the modeled output covariance matrix $\mathbf{R}^{oc}$ [cf. (15)] as a function of the tapered slot antenna array size (i.e., the number of antenna elements, N_{el}). All outputs are used for fitting, and the results are shown for various numbers of CBFPs.

function is expected to be dominant in modeling the EEP. The scaling constant C is chosen to approximately match the gain in the observations. This initial choice also ensures that the minimization yields a physically meaningful result. Furthermore, to ease the minimization, we searched for real-valued expansion coefficients only, which already give sufficiently accurate results as indicated by Figs. 1 and 2.

The method does work for complex-valued expansion coefficients, however, there exists a phase ambiguity for the case of incoherent reference sources. For instance, for θ-polarized reference sources, the 2×2 source coherency matrix $\mathbf{E}^i (\mathbf{E}^i)^H$ in (8) has only one real-valued element corresponding to the power of the incident source field. Because we measure the powers of incoherent source fields, one can calibrate for the amplitude of the beam pattern only, even though the relative phase difference between the antenna output signals can be modeled for each received source field. The phase variation of each EEP follows from the summed basis function patterns, however, not in an unambiguous manner if one solves for complex-valued expansion coefficients for incoherent source fields. The phase ambiguity disappears by choosing real-valued expansion coefficients, so that the relative phase difference between the basis function patterns for each element is fixed and set to zero. Limiting to real-valued expansion coefficients means that one can compensate for matching errors pertaining to real-valued terminations only. An open question therefore is: how can this phase degeneracy can be broken? One possible solution that has been proposed is to measure on a few additional artificial reference sources whose incident field is given in both amplitude and phase.

To demonstrate the effect of including edge elements in the error minimization, the fitting is performed for a limited number of receiver outputs, i.e., for an $N_{\text{act}} \times N_{\text{act}}$ covariance matrix block. The fitting error is therefore shown as a function of N_{act}. Furthermore, this error is shown for various numbers of CBFPs. It turns out that, as few as 3 CBFPs are needed to predict the antenna covariance matrix down to an error of about 2–3%. However, the results also demonstrate that, if $N_{\text{act}} \to N$, i.e., if

edge-element are included in the fitting, the basic assumption that all EEPs are identical ceases to hold. This is manifested by the rapid increase in the fitting error for $N_{\text{act}} > 8$, particularly for the strongly-coupled TSAs in Fig. 2. Hence, and as expected, the accuracy increases for larger arrays (smaller edge-truncation effects). A further improvement may be possible by different optimization algorithms which specifically solve for the structure in (15) (possibly semi-analytical), or by more general particle swarm optimizers (see e.g. [14], [15]).

Fig. 3 confirms the above hypothesis that, as the array size increases (larger N_{el}), the fitting error of the output covariance matrix generally decreases. This can be understood by realizing that the proposed method is entirely founded on the assumption that all embedded element patterns are identical. Indeed, our method essentially implies that the array beam can be modeled by an array factor multiplied by a single unknown embedded element pattern which is expanded in terms of a few relatively slowly varying CBFPs. Note, however, that the error ϵ does not decrease monotonically as N_{el} increases, which may be caused by the mechanism of field interference across the face of the array which differs for different array sizes (array truncation effects). Furthermore, and in accordance with Figs. 1 and 2, one can observe that the fitting error decreases if more CBFPs are employed.

Fig. 4(a) and (b) show the actual and resulting modeled power far-field patterns when the array beam is scanned to $\theta = 30°$. In addition, the relative local gain difference (RLGD) is shown for both the 11-element dipole and TSA arrays. The RLGD is computed as the absolute local gain difference relative to the global maximum gain. The modeled beams pertain to the cases where a single (primary) CBFP and the larger sets of 3 and 5 CBFPs are employed. It is observed that by employing only 3 CBFPs, the RLGD reaches a level which is smaller than -40 dB for the dipole array, and -30 dB for the TSA array, over the entire range of observation angles. Increasing the number of secondary CBFPs does not lead to an improved accuracy, because we have reached the point beyond which the EEPs cannot be regarded identical anymore. This effect is more pronounced
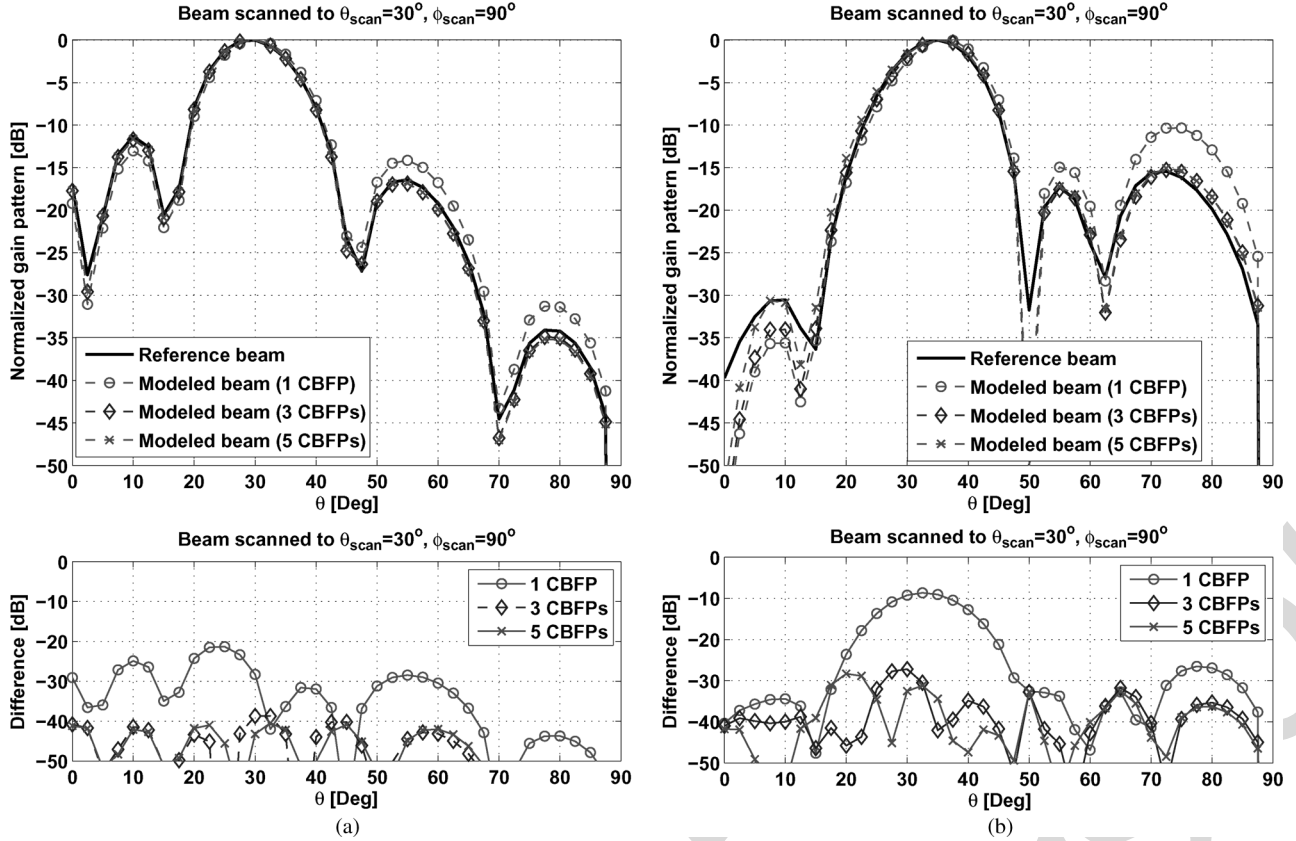
Fig. 4. Reference and modeled normalized array power gain patterns for various numbers of employed CBFPs, for (a) the 11-element dipole antenna array (30° scan in the H-plane); (b) the 11-element tapered slot antenna array (30° scan in the E-plane). The power gain pattern difference is computed relative to the maximum pattern gain.

for the TSA array, which support our conclusions on the validity of the proposed method. Another interesting observation is that the beam-pointing error has been correctly predicted in Fig. 4. At this point, one can adjust the weights to compensate for this error (calibration).

VI. SOLUTION STABILITY

It is important to examine the solution stability of the expansion coefficient vector $\boldsymbol{\alpha}$ as a function of the location of the sky reference sources for a given set of basis function patterns (CBFPs). Toward this end, we recall the analogous situation that, in a method-of-moment approach, the unknown current is expanded in M known basis functions and the integral equation is tested M times to yield a matrix equation which can be solved for the unknown expansion coefficient vector. The matrix condition number is then a measure for the solution stability, which depends on the chosen basis and test functions [4, pp. 41–44]. Note the similarity with the herein proposed method, where each radiation pattern (EEP) is expanded in terms of M CBFPs and where the (least-squares) residual pattern error is measured (tested) in several different directions using $r \geq M$ point sources in the sky (point matching). Also, and as opposed to solving a linear matrix equation as in conventional MoM approaches, the unknown expansion coefficient vector $\boldsymbol{\alpha}$ is determined by solving the non-linear covariance-matrix-fitting problem (15) whose solution is not known in closed form.

For the present stability analysis, we therefore reduce the non-linear fitting problem (of complex correlator output powers) to a linear one (of complex antenna output voltages) and assess the solution stability of $\boldsymbol{\alpha}$ through the matrix condition number. The penalty for not fitting at once to a rank r covariance matrix for r incoherent perfectly-polarized sources (as done above), is that we must now measure the antenna output voltage vector for each source at a time. Nonetheless, the qualitative observations/conclusions for the actual non-linear fitting problem in (15) are believed to be similar to the linear fitting problem insofar the effect of the position of sky reference sources on the solution stability is concerned.

Consider a hypothetical infinite array of radiators placed a distance $\lambda_0/2$ apart along the y-axis (similar to Fig. 1), each having the same $\cos(\theta)$-type of EEP. The r incoherent sky reference sources are x-polarized and located in the $\phi = \pi/2$ plane at $\theta = \{\Delta\theta, 2\Delta\theta, \ldots, M\Delta\theta\}$. In addition, a total of $M \leq r$ CBFPs are employed for the EEP, whose set is found through (4), i.e.,

$$\{g_{x;m}\}_{m=1}^M = \left\{\cos(\theta)e^{j\pi\left(\frac{M+1}{2}-m\right)\sin(\theta)}\right\}_{m=1}^M \tag{16}$$

for $M \in \{3, 5, 7, \ldots\}$ and $\phi = \pi/2$. Note that $g_x = \cos(\theta)$ for $M = 1$.

In the receiving situation (cf. Section III), the pth open-circuited port voltage is defined as $V_p^{\mathrm{oc}} = (j\omega\mu_0)^{-1}\boldsymbol{f}_p(\Omega_m) \cdot \boldsymbol{E}^{\mathrm{i}}(\Omega_m)$, where $\boldsymbol{f}_p = \sum_{m=1}^M \alpha_m g_{x;m}(\theta_m)\hat{\boldsymbol{x}}$ is the modeled
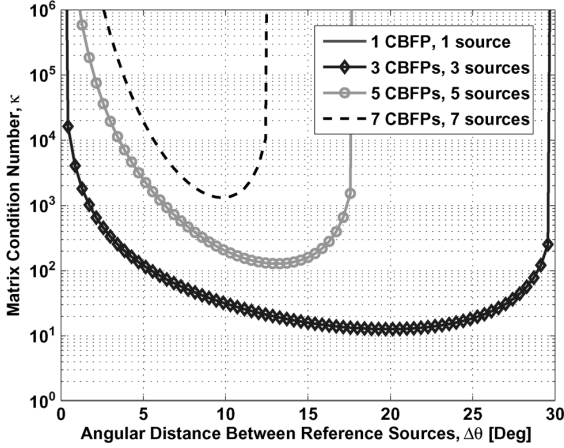
Fig. 5. Matrix condition number κ of the matrix **A** for determining the expansion coefficient vector α as a function of the number of point sources and their angular separation distance.

transmit pattern of the pth antenna element in the source direction θ_m, and $\boldsymbol{E}^{\mathrm{i}} = \hat{\boldsymbol{x}}$. Next, the r modeled receive voltages for each source direction can be least-squares-fit to the measured ones to obtain the M expansion coefficients. To this end, we solve

$$\mathbf{A}\boldsymbol{\alpha} = \mathbf{V} \qquad (17)$$

where the matrix **A** is of size $r \times M$ whose elements are given as

$$A_{sm} = (j\omega\mu_0)^{-1} g_{x;m}(\theta_s) \qquad (18)$$

for $s = 1, \ldots, r$ and $m = 1, \ldots, M$. The vector $\boldsymbol{\alpha}$ is of size $M \times 1$, and the elements of the measured voltage vector **V** of size $r \times 1$ are given as

$$V_s = V_p(\theta_s) \qquad (19)$$

which are the output voltages of the pth element, measured consecutively for each source direction. The solution of (17) is given through the Moore-Penrose pseudoinverse [16]

$$\boldsymbol{\alpha} = \left(\mathbf{A}^H \mathbf{A}\right)^{-1} \mathbf{A}^H \mathbf{V}. \qquad (20)$$

In our example, we choose that $M = r$ and we consider the condition number κ of **A**. Generally, for non-square matrices **A**, one could consider the ratio of the largest singular value to the smallest one. The condition number normally improves for more sources than basis functions, so we limit ourselves to the case that $M = r$. The results are shown in Fig. 5 for 1, 3, 5, and 7 CBFPs or sources as a function of the source separation distance $\Delta\theta$.

Clearly, for $M > 1$ CBF or source, and as the sky reference sources start to cluster (smaller $\Delta\theta$), the matrix condition number increases. Consequently, the stability of the solution deteriorates which causes the solution accuracy of $\boldsymbol{\alpha}$ to decrease. As a result, the calibration accuracy may decrease rapidly depending upon the system noise level. Generally, the problem is better conditioned for well-separated sources. Furthermore, the matrix condition number improves for fewer sources or CBFPs,

however; the improved solution stability is traded against a decreased solution accuracy if fewer CBFPs are employed (see e.g. Fig. 1). Finally, for the case of M sources or CBFPs, and for $\Delta\theta = 90/M$ degrees, one source is placed exactly in the null of all basis function patterns, $\cos(\theta) = 0$, as a result of which the problem cannot be solved uniquely. Hence, one should prevent to measure sources near pattern nulls for improved stability, particularly if the number of sources is not much larger than the number of CBFPs (i.e., for weakly overdetermined systems).

VII. CONCLUSIONS AND RECOMMENDATIONS

A novel method has been proposed to model the antenna array far-field pattern by a superposition of physics-based basis function patterns, called CBFPs. The expansion coefficients are determined experimentally through a single far-field measurement. In this paper, the proposed expansion method is applied to aperture phased array antennas. If edge-truncation effects are negligible, all embedded element patterns (EEPs) are identical, apart from a phase transformation. Accordingly, CBFPs can be employed for expanding the (average) EEP, while the element positions are incorporated in an array factor. It has been demonstrated for an 11-element array of dipoles and arrays of strongly-coupled tapered slot antennas that only 3 CBFPs are sufficient to achieve a 2–3% least-squares fitting error of the modeled to the reference output voltage covariance matrix. Furthermore, the computed resulting array beam exhibits a local gain error smaller than -30 dB relative to the global gain maximum. The accuracy increases for arrays with smaller edge-truncation effects (larger array size, sparser). We concluded from the stability analysis of the expansion coefficient vector that the clustering of sky reference sources should be avoided and that the location of sources should not coincides with the nulls of the CBFPs, particularly for weakly overdetermined systems.

It has been shown that CBFPs are particularly well suited to model beams that are radiated by antenna arrays. Future research directions include: (i) the generation of separate edge-element CBFPs to further increase the beam modeling accuracy; (ii) the development of dedicated optimization solvers for determining the expansion coefficients; (iii) to apply the proposed method in resolving the unitary matrix ambiguities for unpolarized sources, and; (iv) to extend the method to phased array feeds for reflector antennas, where each CBFP is generated from an aperture source distribution, which results from a primary EEP illuminating the reflector. In the latter case it is natural to represent each CBFP, in turn, by Jacobi and Fourier-Bessel series expansions with fixed expansion coefficients to ease the pattern interpolation.

Finally, we conclude that the proposed technique is potentially capable of speeding up array calibration by one or two orders of magnitude, which is beneficial for applications such as astronomical receivers where antenna radiation characteristics are subject to drifts and must be periodically remeasured to accurately calibrate the instrument.

REFERENCES

[1] H. L. van Trees, *Optimum Array Processing—Part IV of Detection, Estimation, and Modulation Theory*. New York: Wiley, 2002.

[2] M. V. Ivashina, O. Iupikov, R. Maaskant, W. A. van Cappellen, and T. Oosterloo, "An optimal beamforming strategy for wide-field surveys with phased-array-fed reflector antennas," *IEEE Trans. Antennas Propag.*, vol. 59, no. 6, pp. 1864–1875, Jun. 2011.

[3] V. Prakash and R. Mittra, "Characteristic basis function method: A new technique for efficient solution of method of moments matrix equations," *Microw. Opt. Technol.*, vol. 36, pp. 95–100, Jan. 2003.

[4] R. Maaskant, "Analysis of Large Antenna Systems" Ph.D. dissertation, Eindhoven University of Technology, Eindhoven, 2010 [Online]. Available: http://alexandria.tue.nl/extra2/201010409.pdf

[5] W. A. van Cappellen, S. J. Wijnholds, and J. D. Bregman, "Sparse antenna array configurations in large aperture synthesis radio telescopes," in *Proc. 3rd European Radar Conf.*, Manchester, UK, Sep. 2006, pp. 76–79.

[6] S. van der Tol, B. D. Jeffs, and A.-J. van der Veen, "Self-calibration for the LOFAR radio astronomical array," *IEEE Trans. Signal Process.*, vol. 55, no. 9, pp. 4497–4510, Sep. 2007.

[7] S. J. Wijnholds, "Fish-Eye Observing With Phased Array Radio Telescopes," Ph.D. dissertation, Delft University of Technology, Delft, 2010.

[8] Y. Rahmat-Samii and V. Galindo-Israel, "Shaped reflector antenna analysis using the jacobi-bessel series," *IEEE Trans. Antennas Propag.*, vol. 28, no. 4, pp. 425–435, Jul. 1980.

[9] K. F. Warnick, M. V. Ivashina, S. J. Wijnholds, and R. Maaskant, "Polarimetry with phased array antennas: Theoretical framework and definitions," *IEEE Trans. Antennas Propag.*, vol. 60, no. 1, pp. 184–196, Jan. 2012.

[10] R. E. Collin and F. J. Zucker, *Antenna Theory—Part 1*. New York and London: McGraw-Hill, 1969.

[11] J. P. Hamaker, "Understanding radio polarimetry—IV. The full-coherency analogue of scalar self-calibration: Self-alignment, dynamic range and polarimetric fidelity," *Astron. Astrophys. Suppl. Ser.*, vol. 143, no. 3, pp. 515–534, May 2000.

[12] R. Maaskant and B. Yang, "A combined electromagnetic and microwave antenna system simulator for radio astronomy," in *Proc. Eur. Conf. on Antennas and Propag. (EuCAP)*, Nice, France, Nov. 2006, pp. 1–4.

[13] R. Maaskant, M. V. Ivashina, O. Iupikov, E. A. Redkina, S. Kasturi, and D. H. Schaubert, "Analysis of large microstrip-fed tapered slot antenna arrays by combining electrodynamic and quasi-static field models," *IEEE Trans. Antennas Propag.*, vol. 56, no. 6, pp. 1798–1807, Jun. 2011.

[14] S. Wan, P.-J. Chung, and B. Mulgrew, "Near-field array shape calibration," in *Proc. Int. Conf. on Acoustics, Speech, and Signal Processing (ICASSP)*, Prague, Czech Republic, May 2011, pp. 2564–2567.

[15] B. Birge, "PSOT—A particle swarm optimization toolbox for use with Matlab," in *Proc. Swarm Intelligence Symp. (SIS'03)*, Indianapolis, IN, Apr. 2003, pp. 182–186.

[16] E. H. Moore, "On the reciprocal of the general algebraic matrix," *Bull. Amer. Math. Society*, vol. 26, no. 9, pp. 394–395, 1920.

Marianna V. Ivashina (M'11) received the Ph.D. degree in electrical engineering from the Sevastopol National Technical University (SNTU), Ukraine, in 2000.

From 2001 to 2004, she was a Postdoctoral Researcher and, from 2004 to 2010, an Antenna System Scientist at The Netherlands Institute for Radio Astronomy (ASTRON). During this period, she carried out research on an innovative phased array feed (PAF) technology for a new-generation radio telescope, known as the square kilometer array (SKA). The results of these early PAF projects have led to the definition of APERTIF—a PAF system that is being developed at ASTRON to replace the current horn feeds in the Westerbork Synthesis Radio Telescope (WSRT). She was involved in the development of APERTIF during 2008–2010 and acted as an external reviewer at the Preliminary Design Review of the Australian SKA Pathfinder (ASKAP) in 2009. In 2002, she also stayed as a Visiting Scientist with the European Space Agency (ESA), ESTEC, The Netherlands, where she studied multiple-beam array feeds for the satellite telecommunication system large deployable antenna (LDA). She is currently a Senior Scientist at the Department of Earth and Space Sciences (Chalmers University of Technology). Her interests are wideband receiving arrays, antenna system modeling techniques, receiver noise characterization, signal processing for phased arrays, and radio astronomy.

Dr. Ivashina received the URSI Young Scientists Award for the GA URSI, Toronto, Canada (1999), an APS/IEEE Travel Grant, Davos, Switzerland (2000), the 2nd Best Paper Award ("Best Team Contribution") at the ESA Antenna Workshop (2008) and the International Qualification Fellowship of the VINNOVA—Marie Curie Actions Program (2009) and The VR project grant of the Swedish Research Center (2010).

Stefan J. Wijnholds (S'06–M'10) was born in The Netherlands in 1978. He received the M.Sc. degree in astronomy and the M.Eng. degree in applied physics (both *cum laude*) from the University of Groningen, The Netherlands, in 2003, and the Ph.D. degree (*cum laude*) from Delft University of Technology, Delft, The Netherlands, in 2010.

After his graduation in 2003, he joined the R&D Department, ASTRON, the Netherlands Institute for Radio Astronomy, Dwingeloo, where he works with the system design and integration egroup on the development of the next generation of radio telescopes. From 2006 to 2010, he was also affiliated with the Delft University of Technology, Delft. His research interests lie in the area of array signal processing, specifically calibration and imaging, and system design of the next generation of radio telescopes.

Dr. Wijnholds received travel grants for the URSI GASS 2008 in Chicago (Ill.), the Asia-Pacific Radio Science Conference in Toyama, Japan (2010) and the URSI GASS 2011 in Istanbul, Turkey.

Rob Maaskant (M'11) was born in the Netherlands on April, 14, 1978. He received the M.Sc. (*cum laude*) and Ph.D. (*cum laude*) degrees in electrical engineering from the Eindhoven University of Technology, Eindhoven, The Netherlands, in 2003 and 2010, respectively.

From 2003 to 2010, he was employed as an Antenna Research Scientist at the Netherlands Institute of Radio Astronomy (ASTRON). He is currently a Postdoctoral Researcher in the Antenna Group, Chalmers University of Technology, Sweden, for which he won a Rubicon postdoctoral fellowship from the Netherlands Organization for Scientific Research (NWO), 2010. He is the primary author of the CAESAR software; an advanced integral-equation based solver for the analysis of large antenna array systems. His current research interest is in the field of receiving antennas for low-noise applications, meta-material based waveguides, and computational electromagnetics to solve these types of problems.

Dr. Maaskant's Ph.D. was awarded "Best Dissertation of the Electrical Engineering Department, in 2010." He received the 2nd best paper prize ("Best Team Contribution") at the 2008 ESA/ESTEC workshop, Noordwijk, and was awarded a Young Researcher Grant from the Swedish Research Council (VR), in 2011.

Karl F. Warnick (SM'04) received the B.S. degree (*magna cum laude* with University Honors) and the Ph.D. degree from Brigham Young University (BYU), Provo, UT, in 1994 and 1997, respectively.

From 1998 to 2000, he was a Postdoctoral Research Associate and Visiting Assistant Professor in the Center for Computational Electromagnetics, University of Illinois at Urbana-Champaign. Since 2000, he has been a faculty member in the Department of Electrical and Computer Engineering, BYU, where he is currently a Professor. In 2005 and 2007, he was a Visiting Professor at the Technische Universität München, Germany. He has published many scientific articles and conference papers on electromagnetic theory, numerical methods, remote sensing, antenna applications, phased arrays, biomedical devices, and inverse scattering, and is the author of the book *Problem Solving in Electromagnetics, Microwave Circuits, and Antenna Design for Communications Engineering* (Artech House, 2006) and coauthor of *Numerical Analysis for Electromagnetic Integral Equations* (Artech House, 2008) and *Numerical Methods for Engineering: An Introduction Using MATLAB and Computational Electromagnetics Examples* (Scitech, 2010).

Dr. Warnick was a recipient of the National Science Foundation Graduate Research Fellowship, Outstanding Faculty Member award for Electrical and

Computer Engineering (2005), and the BYU Young Scholar Award (2007). He has served the Antennas and Propagation Society as a member of the Education Committee and as a session chair and special session organizer for the International Symposium on Antennas and Propagation and other meetings affiliated with the Society. He is a frequent reviewer for the IEEE TRANSACTIONS ON ANTENNAS AND PROPAGATION and *Antennas and Wireless Propagation Letters*. He has been a member of the Technical Program Committee for the International Symposium on Antennas and Propagation for several years and served as Technical Program Co-Chair for the Symposium in 2007.